1   ***Foxtail mosaic virus*: A New Viral Vector for Protein Expression in Wheat and Maize**
2
3   **Clément Bouton[1], Robert C. King[2], Hongxin Chen[1], Kasi Azhakanandam[3], Stéphane Bieri[4], Kim**
4   **E. Hammond-Kosack[1] and Kostya Kanyuka[1]***
5
6   [1]Biointeractions and Crop Protection, Rothamsted Research, Harpenden AL5 2JQ, United Kingdom
7   (C.B., H.C., K.H-K., K.K.); [2]Computational and Analytical Sciences, Rothamsted Research,
8   Harpenden AL5 2JQ, United Kingdom (R.C.K.); [3]Seeds Research, Syngenta Biotechnology Inc.,
9   Research Triangle Park, NC 27709, USA (K.A.); [4]Syngenta Crop Protection AG, CH-4332 Stein,
10   Switzerland (S.B.)
11
12
13
14
15   **Short title:** Virus-mediated protein overexpression in cereals
16
17   **One sentence summary:**
18   A new FoMV vector allows rapid expression of heterologous proteins of up to 600 amino acids in
19   length in wheat and maize
20
21
22
23   **Footnotes**
38

39   **ABSTRACT**

40   Rapid and cost-effective virus-derived transient expression systems for plants are invaluable in
41   elucidating gene function. These are particularly useful in the case of plant species for which
42   transformation-based methods are either not yet developed, or are too time- and labor-demanding,
43   such as wheat and maize. The Virus-mediated overexpression (VOX) vectors based on *Barley stripe*
44   *mosaic virus* (BSMV) or *Wheat streak mosaic virus* (WSMV) previously described for these species
45   are incapable of expressing free recombinant proteins >150-250 amino-acids (aa), not suited for high
46   throughput screens, and have other limitations. In this study, we report the development of a new
47   VOX vector based on a monopartite single-stranded positive sense RNA virus, *Foxtail mosaic virus*
48   (FoMV, genus *Potexvirus*). The gene of interest is inserted downstream of the duplicated sub-
49   genomic promoter of the viral coat protein gene and the corresponding protein is expressed in its free
50   form. This new vector, PV101, allowed expression of a 239 aa-long green fluorescent protein (GFP) in
51   both virus inoculated and upper uninoculated (systemic) leaves of wheat and maize, and directed
52   systemic expression of a larger ca. 600 aa protein GUSPlus in maize. Moreover, we demonstrated
53   that PV101 can be used for *in planta* expression and functional analysis of apoplastic pathogen
54   effector proteins such as host-specific toxin ToxA of *Parastagonospora nodorum*. Therefore, this new
55   VOX vector opens new possibilities for functional genomics studies in two of the most important
56   cereal crops.

57

58

59   **INTRODUCTION**

60   A rapid increase in the use of next generation genome and transcriptome sequencing technologies
61   has facilitated the identification of long lists of candidate genes underlying traits of specific interest in
62   plants and plant-associated organisms. These genes require functional characterization and,
63   therefore, there has been an increasing demand for transient *in planta* expression systems that allow
64   rapid and cost-effective expression of recombinant proteins or RNA interference (RNAi)/silencing of
65   endogenous plant genes.

66   Transient *in planta* expression systems using plant virus vectors, known as VOX (<u>V</u>irus-mediated
67   <u>o</u>ver<u>ex</u>pression), can provide rapid production of heterologous recombinant proteins. Many plant
68   viruses and primarily those with (+) sense single strand (ss) RNA genomes have been cloned and
69   modified to express foreign peptides and proteins *in planta*. One system that is frequently used is
70   *Potato virus X* (PVX, genus *Potexvirus*) (Chapman et al., 1992) and the model dicot species *Nicotiana*
71   *benthamiana.* Important uses of VOX vectors include the investigation and manipulation of metabolic
72   pathways (Majer et al., 2017), functional characterization of host disease resistance genes and
73   pathogen effector proteins (Manning et al., 2010), and cellular protein localization studies (Zhang et
74   al., 2013).

75   Plant (+) ssRNA viruses have also been modified as vectors and used extensively for transient RNAi
76   in a procedure known as VIGS (<u>V</u>irus-<u>i</u>nduced <u>g</u>ene <u>s</u>ilencing), which exploits an endogenous anti-
77   viral RNAi machinery to down-regulate expression of endogenous plant genes. Up until recently only
78   one plant virus has been extensively used for VIGS in wheat, namely *Barley stripe mosaic virus*
79   (BSMV) (reviewed in Lee et al., 2012). The same virus has also been adapted for VOX (Lee et al.,
80   2012; Xu et al., 2015). Although BSMV-mediated VIGS and VOX in wheat work well, these vector
81   systems have several limitations. First, BSMV has a tripartite RNA genome consisting of RNAs α, β
82   and γ, all of which need to be present in the same plant cell to initiate infection. Heterologous genes or
83   gene fragments are usually inserted into RNAγ for expression. The tripartite genome and a need to
84   combine all three genomic RNA for plant inoculation makes the BSMV-expression system only
85   relatively low throughput. Second, as reported by different authors and confirmed in our laboratory,
86   BSMV vectors carrying inserts larger than 450-500-bp are relatively unstable and may also show
87   reduced accumulation and cell-to-cell and systemic movement in the infected plants. Although this
88   size constraint may not be a problem for VIGS, this limits the application of VOX for expression of
89   only relatively small (≤150-aa) proteins reducing a range of possible VOX applications. Third, BSMV
90   induces conspicuous, sometimes moderate to severe chlorotic/necrotic mosaic symptoms (depending
91   on the host genotype), which is undesirable and can hinder the phenotypic assessment of host plants,
92   especially when investigating cell-death related genes and pathways. Fourth, BSMV-VOX only allows
93   production of recombinant proteins as direct C-terminal fusions with the viral γb protein. Although
94   some fusion-free heterologous protein can be obtained by the introduction of the self-cleaving 2A

95 peptide immediately downstream of γb, the cleavage is rarely complete, and fusion-related co-
96 translational processing may interfere with protein's localization and/or intrinsic activity.

97 Two viruses in the family *Potyviridae*, namely *Wheat streak mosaic virus* (WSMV) and *Triticum*
98 *mosaic virus* (TriMV), have been engineered to express fluorescent reporter proteins GFP and RFP
99 allowing monitoring virus spread throughout the infected tissues in wheat and maize and enabling
100 fundamental studies on virus infection biology and on mechanisms of disease resistance (Choi et al.,
101 2000; Tatineni et al., 2015). Only TriMV allowed expression of soluble GFP and RFP (Tatineni et al.,
102 2015), while heterologous proteins produced using WSMV often formed dense aggregate-like
103 structures (Tatineni et al., 2011), which may be undesirable. Although WSMV- and TriMV-directed
104 protein expression is efficient and stable, these viruses have not found a wide use as vectors because
105 of the precise engineering required for inserting a gene of interest into the viral genome and the
106 severity of symptoms induced. Potyviral genomes encode a single long polypeptide, which is then
107 processed into ten mature proteins by virus-encoded proteinases. The foreign genes need to be
108 engineered into genomes of these viruses in frame with the long polypeptide coding open reading
109 frame (ORF) and contain at both the 5'- and 3'-flanks the sequences encoding proteinase cleavage
110 sites required for release of the heterologous proteins from the polyprotein. Processing of these
111 proteins from the polypeptide is not fully efficient resulting in about 10% of the protein present as a
112 fusion with other viral proteins (Tatineni et al., 2011). Moreover, both vectors can only be inoculated
113 onto plants as *in vitro* produced capped transcripts, a methodology that is costly and low throughput.

114 There has also been a report of the monopartite potexvirus, *Foxtail mosaic virus* (FoMV), engineered
115 as a deconstructed vector for protein expression in plants (Liu and Kearney, 2010). This vector was
116 unable to spread systemically and allowed protein expression only in the primary inoculated leaves.
117 Moreover, its efficiency in six different tested monocot species, including wheat and maize, was
118 shown to be negligible (Liu and Kearney, 2010). Recently, two groups reported development of full
119 virus vectors based on FoMV for VIGS in several monocot species. One of these vectors was tested
120 and shown to be efficient for VIGS in maize, sorghum (*Sorghum bicolor*) and green foxtail (*Setaria*
121 *viridis*) (Mei et al., 2016), and another - in barley, foxtail millet (*Setaria italica*), and wheat (Liu et al.,
122 2016). One of the key advantages of these new vectors, in addition to being based on a virus with the
123 monopartite genome, is that FoMV induces no or very mild symptoms. In this study, we report a new
124 vector based on FoMV for VOX in the major cereal crops such as wheat and maize, which overcomes
125 the limitations of the existing expression vectors discussed above.

126

127

128 **RESULTS**

129 **Construction of the first-generation FoMV vectors for protein expression in plants**

130 The first generation binary FoMV VOX vectors were derived from the full-length FoMV cDNA clone
131 pCF (Yau-Heiu Hsu, unpublished). The complete *Potato virus X* (PVX) genome in the VIGS vector
132 pGR106, based on a compact binary expression vector pGreen0000 (Lu et al., 2003), was replaced
133 with the full length FoMV genome from the cDNA clone pCF. The resulting binary plasmid pGR-
134 FoMV.pCF, was transformed into *Agrobacterium tumefaciens* and co-infiltrated into *N. benthamiana*
135 leaves with a strain of *A. tumefaciens* carrying a standard non-viral binary vector for expression of the
136 *Tomato bushy stunt virus* (TBSV) p19 protein, a well-known suppressor of RNA silencing. Very mild
137 chlorosis was observed in the newly emerging upper leaves of all plants from 10 days post infiltration
138 (dpi) onward (Figure 1). The identity of the disease-causing agent in these symptomatic plants as
139 FoMV was confirmed using RT-PCR with primers targeting a 133-nt fragment located in the FoMV
140 ORF1 (Figure 1). Therefore, pGR-FoMV.pCF was directly infectious when introduced to *N.*
141 *benthamiana* plants by agroinfiltration. Agroinfiltrated leaves collected from these plants at 6-dpi
142 served as a FoMV inoculum for mechanical inoculation of young seedlings of wheat cv. Riband. The
143 newly developing leaves of virus inoculated wheat plants exhibited pale green/yellowish chlorotic
144 streaks along the leaf blade (i.e. mild mosaic) from 10-dpi onward, and the presence of FoMV in these
145 leaves was confirmed by RT-PCR (Figure 1).

146 Generation of subgenomic RNAs (sgRNAs) is a mechanism used by many plant viruses with
147 multicistronic (+) ssRNA genomes for expression of their 3'-proximal cistrons (Sztuba-Solińska et al.,
148 2011). Production of sgRNAs is controlled by the *cis*-acting promoter-like elements known as
149 subgenomic promoters (sgps). One of the successful strategies used for expression of heterologous
150 proteins from genomes of viruses in the genus *Potexvirus* involves placing the heterologous

151 sequence downstream of a duplicated viral coat protein (CP) sgp (Chapman et al., 1992; Lin et al.,
152 2004; Sempere et al., 2011; Zhang et al., 2013). Foxtail mosaic potexvirus (FoMV) is known to
153 synthesize two sgRNAs, sgRNA1 and sgRNA2, for expression of ORF2 – ORF4 (encode viral
154 movement proteins) and ORF5/CP (encodes viral coat protein, CP), respectively (Figure 2). Although
155 the precise 5' and 3' boundaries of FoMV CP sgp (designated as sgp2) have not been experimentally
156 defined, an 8nt-long GUUAGGGU core element conserved in CP sgp of other potexviruses (Dickmeis
157 et al., 2014) is present upstream of ORF5/CP in FoMV. Using this core element as a landmark, we
158 selected four different sized sequences ranging from 45- to 101-nt in length encompassing the core
159 sgp2 element for duplication (Figure 2; Figure S1). A multiple cloning site (MCS) containing cut sites
160 for *Sal*I, *Cla*I, *Asc*I, *Hpa*I, and *Xba*I was engineered downstream of the first sgp2 copy, sgp2.1 (Figure
161 2), enabling a restriction enzyme-based insertion of a gene of interest for *in planta* expression. In the
162 case of the two longer sequence duplications (i.e. 90- and 101-nt long) containing a 5'-portion of
163 ORF5/CP, the CP start codon present in sgp2 was eliminated by single nucleotide mutagenesis that
164 converted ATG to AGG, thus ensuring no translation of proteins other than the heterologous protein
165 from sgRNA2.1 (Figure 2). The four resulting expression vectors were named pCF45, pCF55, pCF90,
166 and pCF101. In addition, ORF5A, which initiates 143 nucleotides upstream of the CP and codes for
167 an N-terminally extended variant of CP that is dispensable for systemic infection (Robertson et al.,
168 2000), was disrupted in each of the four FoMV expression vectors due to insertion of MCS. All four
169 vectors were infectious (data not shown).

170

Heterologous proteins can be expressed from the duplicated FoMV sgp2

172 The green fluorescent protein coding gene *GFP (S65T)* (Heim et al., 1995) was inserted into each of
173 the four developed FoMV VOX vectors using restriction enzyme-mediated cloning. The resulting
174 constructs were transformed into *A. tumefaciens* and then co-agroinfiltrated into *N. benthamiana*
175 leaves with an Agrobacterium culture carrying a plasmid for expression of TBSV p19. At 6-dpi, GFP
176 fluorescence was observed under a blue light in all infiltrated leaves in two independent experiments
177 (Figure 3), whereas no fluorescence was detected in leaves infiltrated with the empty vectors or with
178 the TBSV p19-expressing Agrobacterium culture only (Figure 3). GFP was also detected using
179 immunoblotting in leaves of *N. benthamiana* plants infiltrated with bacterial cultures carrying pCF45-
180 GFP, pCF55-GFP, pCF90-GFP, and pCF101-GFP but not in plants infiltrated with Agrobacterium
181 carrying an empty vector pCF101, the infectious cDNA clone pGR-FoMV.pCF, or TBSV p19 (Figure
182 3). Although each of the four sgp2 duplication could drive the expression of GFP, the highest
183 expression levels were consistently obtained with the 90-nt and 101-nt long duplications. The 101-nt
184 long duplication was selected for all subsequent experiments in this study.

185 The pCF101-GFP-agroinfiltrated *N. benthamiana* leaves harvested at 7-dpi served as a virus
186 inoculum for rub-inoculation of leaf 1 (L1) and L2 of young, two-leaf stage wheat cv. Riband seedlings
187 grown under standard conditions (day/night temperature of 23°C/20°C; 16 h light at ~120 µmol m^{-2} s^{-1};
188 and ~65% relative humidity). GFP fluorescence was observed in the virus inoculated leaves at 8-dpi
189 (Figure 4), but no fluorescence was observed in any of the upper uninoculated leaves and the
190 majority of inoculated plants did not develop any systemic symptoms even after >21-dpi. Temperature
191 is known to be one of the key environmental factors influencing virus infection. For example, it has
192 been previously reported that growing plants at temperatures below 24°C results in a delay in the
193 onset of FoMV induced symptoms (Paulsen and Niblett, 1977). To assess whether growth conditions
194 could influence heterologous protein expression from the FoMV vector, we raised and maintained
195 wheat plants post inoculation with pCF101-GFP either under standard conditions (as above) or under
196 slightly elevated temperature regime (day/night temperature of 26.7°C/21.1°C; 16 h light at ~220 µmol
197 m^{-2} s$^{-1;}$ and ~65% relative humidity). GFP fluorescence observed in the leaves inoculated with
198 pCF101-GFP in two independent experiments was more intense and appeared to cover wider area of
199 leaf blades under the higher temperature conditions (Figure 4). Furthermore, under these warmer
200 conditions sparse fluorescence foci were observed also in the second systemically infected leaf L4
201 (Figure 4) in five out of eight plants inoculated with pCF101-GFP, whereas no systemic fluorescence
202 was detected in the 10 plants inoculated under standard growth conditions. We concluded, that
203 elevated temperature can indeed enhance FoMV-mediated expression of heterologous proteins, and
204 that our first-generation vectors although efficient in expressing GFP in the inoculated leaves of wheat
205 performed unsatisfactory in terms of heterologous protein expression in systemically infected tissues.

206

Construction of the second-generation FoMV vector for improved protein expression in plants

208 The first generation FoMV VOX vectors were based on the pCF cDNA clone derived from the FoMV
209 isolate PV139 that was maintained on barley (Yau-Heiu Hsu, personal communication). Viral cDNA
210 clones are traditionally produced by reverse-transcription of isolated viral genomic RNA followed by
211 insertion of the full-length cDNA genome into a plasmid under control of a prokaryotic or eukaryotic
212 promoter. This methodology does not ensure that the cloned virus genome is as infectious as the
213 starting virus material for several reasons. First, replication of RNA viruses is known to be error-prone
214 and therefore during infection of the host, "clouds" of closely related viral genome sequence variants,
215 known as quasi-species, are generated (Domingo et al., 2012). Therefore, the cloned viral genome
216 may represent one of the sub-optimal genome variants. Second, reverse-transcription is itself an
217 error-prone process and hence unwanted inauspicious mutations can occasionally be introduced
218 during the cDNA synthesis step as well. More recently, small RNA sequencing (sRNA-seq) based
219 approaches have proven to be very valuable for reconstituting full-length viral RNA genomes or
220 identifying new plant viruses (Kreuze, 2014; Seguin et al., 2014). These approaches rely on the fact
221 that virus-infected plants accumulate high levels of virus-derived small interfering RNAs (vsiRNAs)
222 produced through the action of the natural antiviral RNA silencing machinery (Csorba and Burgyán,
223 2016). Therefore, we chose to use sRNA-seq followed by *de novo* sequence reads assembly as an
224 unbiased approach to identify the consensus fittest FoMV isolate PV139 genome variant, hereafter
225 referred to as the master genome, produced in wheat.

226 The starting material for these experiments was lyophilized leaves of sorghum plants infected with the
227 FoMV isolate PV139 that had been maintained on sorghum to prevent contamination with *Wheat*
228 *streak mosaic virus* (WSMV) (Seifers et al., 1999). Inoculation of this virus onto wheat cultivars (cvs.)
229 Riband or Chinese Spring typically induced mild chlorotic mosaic symptoms on the upper
230 uninoculated leaves from 7-10-dpi onward (Figure 5), whereas only sporadic mild chlorotic streaks
231 were observed on the newly emerging leaves of cv. Bobwhite from 14-dpi onward (Figure 5).
232 Therefore, cvs. Chinese Spring and Riband were considered good hosts for maintaining this isolate of
233 FoMV. Total RNA extracted from pooled leaf tissue from the infected cvs. Chinese Spring and Riband
234 plants after the seventh consecutive serial passage was used for sRNA-seq (Figure 5). The
235 consensus FoMV master genomes obtained following assembly of sequence reads corresponding to
236 the 20-24-nt fraction of small RNAs were identical between the two biological replicates. The full-
237 length FoMV genome sequence obtained differed from that of FoMV pCF (also originally derived from
238 PV139) at 85 nucleotide positions located both in cistrons and in noncoding sequences (Table S1).
239 The full-length FoMV cDNA containing a 40 nt-long 3'-terminal poly(A)-tail was produced by gene
240 synthesis and cloned into the backbone of the binary vector pGR106 (replacing the PVX cDNA). The
241 resulting pGR-FoMV.PV139 plasmid was transformed into *A. tumefaciens* and co-agroinfiltrated into
242 *N. benthamiana* leaves with the p19-carrying *A. tumefaciens* strain, as described above. Upper non-
243 infiltrated leaves of these plants developed very mild chlorosis similar to that previously observed for
244 pGR-FoMV.pCF. Agroinfiltrated *N. benthamiana* leaves collected at 6-dpi served as a source of
245 inoculum for rub-inoculation of young 2-leaf stage seedlings of wheat cv. Riband. At 10-dpi all
246 inoculated wheat plants developed systemic mosaic (Figure 5) similar to that induced by the original
247 virus inoculum (i.e. that prepared from the infected wheat leaf tissue sampled post seven rounds of
248 virus passaging through wheat). The presence of FoMV was confirmed by RT-PCR (Figure 5).

249 The pGR-FoMV.PV139 was used for developing a second generation FoMV expression vector using
250 the same methodology as described above for pCF101. A 101-nt long fragment spanning the core
251 FoMV sgp2 sequence was duplicated and a MCS containing recognition sites for *Not*I, *Cla*I, *Asc*I,
252 *Hpa*I, and *Xba*I was inserted downstream of the first sgp2 copy. The resulting vector was named
253 PV101. An empty PV101 was infectious (data not shown) and it was further modified by replacing the
254 vector's MCS with the Gateway cassette to produce a second, prototype vector, PV101gw, which
255 allows insertion of heterologous sequences using recombination-based cloning.

256

257 **The FoMV vector PV101 provides improved expression of heterologous proteins in wheat**

258 The *GFP (S65T)* gene was inserted into the PV101 vector using restriction enzyme-mediated cloning,
259 and the resulting plasmid PV101-GFP was transformed into *A. tumefaciens* and agroinfiltrated into *N.*
260 *benthamiana* leaves. At 7-dpi, GFP fluorescence was observed in the infiltrated leaves under blue
261 light but no fluorescence was detected in leaves infiltrated with an empty vector (Figure 6). At 14-dpi,
262 GFP fluorescence was observed around veins in the upper uninoculated leaves (Figure 6),
263 demonstrating the ability of PV101-GFP to replicate and to move systemically in this plant species.
264 GFP was also detected using immunoblotting in the upper uninoculated leaves of PV101-GFP-
265 infiltrated *N. benthamiana* plants, but not in plants infiltrated with the empty vector PV101 (Figure 6).

266 Wheat cv. Riband seedlings, grown under day/night temperature of 26.7°C/21.1°C and inoculated
267 using sap from leaves of *N. benthamiana* plants agroinfiltrated with PV101-GFP, showed GFP
268 fluorescence in both inoculated and systemically infected leaves (Figure 6). In the inoculated leaves
269 GFP fluorescence was observed from 4-dpi onward and lasted for at least another 10 days (Figure
270 S2). GFP fluorescence was readily detectable in the first two systemically infected leaves, L3 and L4,
271 at 11- and 17-dpi, respectively. And although fluorescence in these PV101-GFP infected leaves was
272 rather patchy (Figure 6), PV101 vector clearly outperformed pCF101 (note a very limited systemic
273 fluorescence observed in leaves of pCF101-GFP infected plants; Figure 4). GFP in systemically
274 infected wheat leaves was also detected by immunoblotting (Figure 6). Considerably less FoMV CP
275 accumulated in the systemically infected leaves of wheat plants inoculated with PV101-GFP
276 compared to those inoculated with an empty vector (Figure 6). This might reflect a better spread of
277 the empty PV101 virus and/or a negative effect of the inserted *GFP* gene on CP expression. To
278 assess accurately the GFP expression levels in the systemically infected wheat leaves and across
279 different individuals we developed a GFP fluorescence scoring system (Figure S3) utilizing a scale
280 from 0 to 4 (with 0 – no GFP fluorescence, and 4 – abundant GFP fluorescence foci). The extent of
281 GFP expression was found to be heterogeneous in different plants and even in different systemically
282 infected leaves of the same plant. Roughly 85% of L3, L4 and L5 emerged post inoculation scored
283 only 0 and 1, with the remaining ~15% showing a score of 2 or 3 (Figure S3). Although L6 and newer
284 leaves showed virus-induced mosaic symptoms, no GFP fluorescence was detected in any of these
285 leaves, indicating that FoMV-GFP was relatively unstable during wheat infection. We then tested
286 performance of PV101-GFP on 36 other wheat cultivars the majority of which had been bred in
287 Europe. Good levels of GFP fluorescence were observed in the inoculated leaves on all the European
288 cultivars assessed (Figure 7; Table S2). Seven cultivars (i.e. ~22% of all tested) including Bobwhite
289 showed no GFP fluorescence and no or very limited systemic mosaic symptoms in any of the
290 assessed inoculated or upper uninoculated leaves, indicating that these cultivars were either partially
291 or fully resistant to PV101-GFP. Whereas the FoMV-locally susceptible cultivars displayed variable
292 maximum levels of GFP fluorescence in the systemically infected leaves, from low (score = 1) and
293 patchy (score = 2) to sometimes almost uniform throughout the entire leaf blades (score = 4) as in cv.
294 Pakito (Figure 7). In summary, our data indicate that FoMV-directed heterologous protein expression
295 is likely to be achieved in many European wheat cultivars whereas at least some of the non-European
296 wheat genotypes may be poor hosts for PV101 under the growth conditions tested.

297 An expression construct produced by recombining coding sequence of *GFP (S65T)* into the Gateway-
298 enabled vector PV101gw, was also fully infectious and GFP expression was detected in the infected
299 plant tissues (Figure S4).

300 Recently a FoMV vector for VIGS has been described (Liu et al., 2016). This vector, pFoMV-sg, was
301 developed through duplication of 170-nt long sequence which encompassed not only sgp2 but also an
302 entire ORF5A located upstream of ORF5/CP. To investigate whether this longer sgp2 duplication may
303 also be suitable for driving expression of heterologous proteins, we constructed an additional vector
304 based on pGR-FoMV.PV139 that contained a 169-nt long duplication of sgp2 equivalent to that in the
305 VIGS vector pFoMV-sg (Figure S5). The resulting vector PV169 could express GFP in both *N.*
306 *benthamiana* and wheat, however the observed GFP fluorescence in the infected leaves was less
307 intense than that in the PV101-GFP infected leaves and the PV169-GFP-infiltrated *N. benthamiana*
308 leaves accumulated less GFP but noticeably more viral CP than the PV101-GFP infiltrated leaves as
309 determined by immunoblotting (Figure S5).

310

311 **The FoMV vector PV101 efficiently expresses heterologous proteins in maize**

312 Next, we assessed whether PV101 can be used for VOX in another major cereal crop, maize (*Zea*
313 *mays*). Young (3-4 leaf stage) seedlings of maize line B73 with a sequenced genome (Schnable et al.,
314 2009) were inoculated by rubbing L1, L2 and L3 with the PV101-GFP-containing sap from infected *N.*
315 *benthamiana* plants as described above. Isolated GFP foci were observed in the systemically infected
316 leaves from 7-dpi and good GFP fluorescence spread was observed from 14-dpi onwards (Figure 6).
317 GFP was readily detected in systemic leaves using immunoblotting (Figure 6). In some maize B73
318 plants GFP fluorescence was detected in all systemically infected leaves up to and including L7 and
319 relatively high GFP fluorescence scores (scores = 3 or 4) were regularly observed (Figure S3).
320 Therefore, maize line B73 appears to be an acceptable good host for FoMV PV139.

321

322 **The FoMV vector PV101 can be used for expression of proteins as large as 600 amino acids**

323 PV101 was tested for *in planta* expression of large proteins. In this experiment, a synthetic *gusA* gene
324 based on the sequence from *Staphylococcus* sp., encoding a 600 amino acids-long protein GUSPlus
325 (Broothaerts et al. 2005), was cloned into PV101. GUSPlus expression was observed in the PV101-
326 GUSPlus-inoculated leaves of both wheat and maize seedlings (Figure 8). GUSPlus expression in the
327 systemically infected wheat leaves appeared to be more limited than expression of GFP (Figure 8).
328 This suggests a negative correlation between insert length and vector stability. Slightly higher levels
329 of GUSPlus expression were observed in the upper uninoculated leaves of wheat cv. Pakito (Figure
330 8), which agrees well with the fact that this same cultivar showed the best GFP fluorescence scores in
331 the systemically infected leaves among all wheat cultivars tested (Figure 7).

332 By contrast to the suboptimal performance of PV101-GUSPlus in the systemically infected wheat
333 leaves, adequate levels of GUSPlus expression were observed in the upper uninoculated maize
334 leaves (Figure 8). The percentage of symptomatic maize plants showing systemic GUSPlus
335 expression varied from 33% to 83% between three independent experiments (Table S3). The best
336 GUSPlus expression levels were consistently observed in L5, with GUS staining less intense and
337 somewhat patchier in L4 and L6 (Figure 8).

338 In conclusion, our study demonstrates that the FoMV vector PV101 can be used to express
339 heterologous proteins of up to 600 amino acids in the inoculated leaves of wheat and maize, and in
340 up to three consecutive systemically infected leaves in maize.

341

342 **The FoMV vector PV101 can be used as a tool for expression of pathogen effector proteins**

343 Functional analysis of genes encoding small secreted effector proteins predicted in the genomes of
344 wheat-infecting fungal pathogens currently relies on labor-intensive methods when assessing their
345 function in wheat. Typical experiments involve expression of candidate effectors in heterologous *in*
346 *vitro* systems (such as the yeast *Pichia pastoris* or *E. coli*) followed by syringe infiltration of purified
347 effectors into wheat leaves and analysis of resulting induced phenotypes/responses. To test the
348 suitability of the new vector for this purpose, we cloned the full-length coding sequence of a well-
349 studied necrotrophic effector ToxA (Friesen et al., 2006; Liu et al., 2006) from *Parastagonospora*
350 *nodorum*, the causal agent of glume blotch disease in wheat, into PV101. ToxA is known to induce
351 necrosis on wheat cultivars carrying the corresponding sensitivity gene *Tsn1* (Friesen et al., 2006;
352 Faris et al., 2010). As expected, only ToxA-sensitive wheat cv. Halberd but not ToxA-insensitive
353 wheat cv. Chinese Spring when inoculated with the PV101-SnToxA construct developed necrosis in
354 both inoculated and systemically infected leaves (Figure 9). A mature version of ToxA (without its
355 native signal peptide) was also cloned into PV101. The resulting PV101-ToxA_noSP induced necrosis
356 in systemic leaves of wheat cv. Halberd only but the necrosis was delayed by at least 5 days in
357 comparison with the necrosis induced by the full length ToxA in two independent experiments. This
358 indicates that secretion of ToxA into the apoplastic space is not absolutely required, which agrees well
359 with the previous work by Manning and Ciuffetti (2005) demonstrating that ToxA is imported within the
360 cell in *Tsn1* wheat lines. PV101-GFP was used as a control in these experiments and induced only
361 mild chlorotic mosaics on both cultivars (Figure 9). We therefore conclude that the new FoMV vector
362 PV101 has great potential for VOX applications such as medium-to-high throughput screens for
363 necrosis or cell-death inducing candidate fungal effectors.

364

365

366 **DISCUSSION**

367 Here we report the development of a new vector, based on the foxtail mosaic potexvirus (FoMV), for
368 expression of heterologous proteins, including large fusion-free proteins of up to 600 amino acid in
369 size and pathogen-secreted effector proteins, for applications in two major crops wheat and maize.
370 This new vector, PV101, induced only mild symptoms on both wheat and maize (as well as in a
371 laboratory dicotyledonous host *N. benthamiana*), which agrees well with findings from studies of
372 FoMV by others (Paulsen and Niblett, 1977; Robertson et al., 2000; Liu et al., 2016; Mei et al., 2016).
373 This lack of strong symptoms is a very useful feature when determining plant phenotypes induced by
374 heterologous proteins, especially those predicted to induce or regulate plant defense, cell death
375 and/or senescence pathways. However, appropriate controls must be included when designing a new
376 VOX experiment since the presence of mild symptoms indicates that some changes in plants'
377 physiology do occur during FoMV infection.

378   The PV101 VOX vector is superior to the existing monocot expression vectors in several other
379   aspects. Specifically, this study shows that PV101 can carry the 1800 nt-long *GUSPlus* gene coding
380   sequence representing an increase of about 30% in the FoMV genome length, whereas BSMV-
381   derived vectors do not tolerate well inserts larger than ~ 450-500 nt (Lee et al., 2012) and potyvirus-
382   derived vectors can stably express only moderately sized proteins such as RFP (237-aa), GFP (238-
383   aa) and neomycin phosphotransferase II (264-aa) but not proteins that are as large as GUS (603-aa)
384   (Choi et al., 2000; Tatineni et al., 2011; 2015). Furthermore, PV101 allows expression of heterologous
385   proteins in their native forms including those with the N-terminal signal sequences for secretion
386   outside the plant cell, whereas heterologous proteins expressed from potyviruses WSMV and TriMV
387   or from BSMV must be processed from polyproteins by the native or heterologous proteases, a
388   process that is only 90% efficient at best. In addition, expression vectors based on FoMV, a
389   potexvirus with the monopartite genome, that utilize a strategy of heterologous protein expression
390   from subgenomic RNA have greater potential for applications requiring higher throughput. As a proof
391   of concept, we engineered a second, prototype FoMV vector, named PV101gw, enabling high-
392   throughput cloning of heterologous sequences using the Gateway recombination technology.
393   Although not yet fully tested for its ability to express a range of different proteins in wheat, this vector
394   was effective in expressing GFP in the infected plant tissues (Figure S4).

395   Two different FoMV vectors for VIGS in monocots, including wheat and maize, have recently been
396   described (Liu et al., 2016; Mei et al., 2016). The pFoMV-V vector (Mei et al., 2016) was designed for
397   cloning the heterologous sequences using the engineered *Xba*I and *Xho*I restriction enzyme
398   immediately downstream of the stop codon of the viral coat protein (CP) ORF. This vector cannot be
399   used for protein expression because the gene of interest, cloned downstream of CP ORF, would be in
400   the second position on the coat protein subgenomic RNA, and therefore would remain silent. Another
401   published FoMV VIGS vector, pFoMV-sg (Liu et al., 2016), was developed using a similar strategy to
402   that used in this study and involved duplication of a predicted sgp2. However, by contrast to PV101
403   bearing a relatively short 101-nt sgp2 duplication, pFoMV-sg contained a 170-nt long duplication,
404   which spanned the sgp2 core sequence as well as a dispensable ORF5A (Liu et al., 2016). Here we
405   showed that this longer duplication of predicted sgp2, although able to direct expression of
406   heterologous proteins, is less effective than the 101-nt sgp2 sequence duplication. The vector,
407   PV169, constructed to replicate the sgp2 duplication in pFoMV-sg, produced less GFP and more viral
408   CP in the inoculated plants than PV101 (Figure S5). It may therefore be concluded, that longer sgp2
409   promoter duplications, as in pFoMV-sg and PV169, somehow confer reduced insert stability. Although
410   insert stability in pFoMV-sg was not specifically investigated in the study by Liu et al. (2016), these
411   authors reported that a 200-bp barley phytoene desaturase (*HvPDS*) DNA fragment cloned into
412   pFoMV-sg induced only a very limited silencing of the endogenous *PDS* in barley whereas 110-120-
413   bp long inserts containing direct inverted repeat fragments of various monocot plant genes induced
414   efficient silencing of targeted endogenes. A more efficient gene silencing with VIGS vectors carrying
415   110-120-bp inserts, may at least in part be explained by their potentially higher stability over those
416   bearing inserts longer than 200-bp.

417   Our current FoMV VOX procedure involves propagation of the PV101-derived constructs in *N.*
418   *benthamiana* prior to their inoculation onto monocot plants. This limits the experimental throughput.
419   Furthermore, avoiding this first step of virus inoculum build-up in *N. benthamiana* may be necessary
420   when testing constructs for expression of generic cell death inducing proteins (Lacomme and Santa
421   Cruz, 1999; Tang et al., 2015; Kettles et al., 2017), predicted proteinaceous pathogen-associated
422   molecular patterns (PAMPs) (Franco-Orozco et al., 2017), or certain candidate pathogen effector
423   proteins that may be recognized by the corresponding immune receptors in this plant species
424   (Dagvadorj et al., 2017; Kettles et al., 2017). We, therefore, assessed a possibility of delivering the
425   FoMV VOX vector directly into wheat leaves using infiltration with a recA-deficient *Agrobacterium*
426   *tumefaciens* strain COR308 harboring a disarmed pTi derivative plasmid pMP90 and a helper plasmid
427   pCH32, which provides extra copies of the *virA* and *virG* genes (Hamilton, 1997), and a
428   corresponding protocol that was claimed to be efficient in delivering BSMV-derived gene silencing
429   constructs directly to wheat leaves (Panwar et al., 2013). However, all our attempts to inoculate
430   directly wheat cvs. Riband and Pakito with PV101-GFP or pGR-FoMV-PV139 using this approach
431   were unsuccessful (data not shown). Other means of direct delivery of virus vectors, in which
432   transcription of the viral genomes is under control of the CaMV 35S promoter, to monocot plants have
433   been reported. For example, micro-projectile particle bombardment was used to deliver BSMV VIGS
434   and VOX vectors (Meng et al., 2009; Xu et al., 2015) and the recently developed pFoMV-V VIGS
435   vector (Mei et al., 2016) directly to barley and maize leaves, respectively. Very recently a new
436   procedure for inducing *Tobacco rattle virus*-mediated VIGS in wheat and maize has been described

437 (Zhang et al., 2017). It involves the use of vacuum infiltration and co-cultivation with Agrobacterium in
438 Luria-Bertani medium supplemented with acetosyringone, cysteine, and Tween 20. Further studies
439 are needed to investigate whether any of the methods described above may be used for direct
440 inoculation of the PV101-derived expression constructs directly to wheat, maize and other monocot
441 crops.

442 Screening a collection of 37 wheat cultivars with PV101-GFP revealed that hexaploid wheat (*Triticum*
443 *aestivum*) is not universally susceptible to FoMV. Some cultivars, largely those of non-European
444 origin, showed partial or complete virus resistance (Figure 7; Table S2). We thus recommend testing
445 the chosen wheat cultivars for their susceptibility to FoMV before planning a new PV101-VOX study.
446 The same applies to the VOX studies involving maize, because some maize inbred lines, e.g. Mo17,
447 have been reported to be resistant to FoMV (Ji et al., 2010; Mei et al., 2016). Maize inbred lines
448 previously shown to be susceptible to pFoMV-V (Mei et al., 2016) are also likely to be susceptible to
449 PV101 because both these vectors originate from the same FoMV isolate, namely PV139.

450 Our main initial objective was to develop a new virus-based expression vector for wheat. Therefore,
451 the FoMV isolate PV139 selected for this study was first passaged several times through wheat, and
452 the VOX vector PV101 was derived from the most highly abundant and hence most likely the fittest
453 FoMV quasi-species accumulating in this experimental host. Nevertheless, somewhat surprisingly,
454 maize was found to be a better systemic host for PV101 than wheat. That is, a nearly uniform GFP
455 fluorescence across the entire leaf blades was more frequently observed in maize plants systemically
456 infected with PV101-GFP than in wheat (Figure S3). Also, expression of a larger protein, GUSPlus,
457 was more stable and noticeably more efficient in maize (Figure 8). These data suggest that FoMV
458 may be naturally better adapted to infect maize than wheat. With this regard, it is interesting to note
459 that FoMV PV139 was originally isolated from *Setaria viridis* and *Setaria italica* growing as weeds in a
460 maize field (Paulsen and Niblett, 1977). Also, FoMV has been previously isolated from *Sorghum*
461 *bicolor* (Seifers et al., 1999). It is quite remarkable that the only natural hosts reported for FoMV as
462 well as seemingly the best experimental host maize all are species with the C_4 photosynthetic
463 pathway. Leaves of C_4 plants have anatomy known as Kranz-type, in which the vascular bundle is
464 surrounded by the organelle-rich vascular bundle sheath cells and this tissue layer further surrounded
465 by the radially arranged mesophyll cells. This anatomy facilitates transport of photosynthetic
466 assimilates between the different cell types. Leaf anatomy of C_3 plants is very different, with the
467 mesophyll cells being well developed relative to the organelle-poor vascular bundle sheath cells.
468 Another key difference between leaves of C_4 and C_3 plants is that C_4 leaves have much denser
469 networks of small longitudinal and transverse veins (Brown and Hattersley, 1989). It seems possible
470 that the leaf anatomy of C_4 plants is more favorable to FoMV spread and ultimately to the vector
471 performance than the anatomy of C_3 plants, e.g. wheat.

472

473

474 **CONCLUSIONS**

475 Here we developed a new FoMV vector PV101 for transient protein expression in wheat in maize and
476 demonstrated successful expression of a wide range of native proteins from 178-aa long (ToxA) to at
477 least ca. 600-aa long (GUSPlus). Although not specifically tested here, it is likely that PV101 can be
478 used for VOX in plants such as *Sorghum bicolor*, *Setaria italica* and *Setaria viridis*, which are natural
479 hosts for FoMV, as well as in several other monocots including important crops such as barley, oat
480 and rye that can be systemically infected with FoMV under laboratory conditions (Paulsen and Niblett,
481 1977). Furthermore, FoMV-mediated VOX using PV101 and PV101gw can be used in medium
482 throughput screens and the vector can be modified further to allow rapid restriction endonuclease
483 independent cloning and thereby increase experimental throughput. This opens a wide range of
484 applications where an easy and rapid method of heterologous protein expression in monocots is
485 needed. For example, PV101 may be used in screens for cell-death activity of secreted or cytosolic
486 candidate pathogen effectors in wheat, maize or other monocot crops or model species, or in screens
487 for proteins with putative insecticide or antifungal activities. We are positive many other interesting
488 and useful applications for PV101 will soon be found by the scientific research community.

489

490

491 **MATERIALS AND METHODS**

Plants and growth conditions

N. benthamiana plants were grown in a controlled environment room with day/night temperature of 23°C/20°C at 60% relative humidity and a 16 h photoperiod with approximately 130 µmol m^{-2} s^{-1} light. Maize (*Z. mays*) and bread wheat (*T. aestivum*) were grown in a controlled environment room with day/night temperature of 26.7°C (80°F)/21.1°C (70°F) at around 65% relative humidity and a 16 h photoperiod with approximately 220 µmol m^{-2} s^{-1} light.

Serial passaging of FoMV isolate PV139 through wheat

Ten to 11-day-old wheat plants of three different wheat cultivars (Chinese Spring, Riband, and Bobwhite) were rub inoculated with the sap prepared by grinding 70 mg freeze-dried FoMV PV139 infected *Sorghum bicolor* (Asgrow XP6105) leaves in 1.5 mL deionized water supplemented with 15 mg coarse Celite 545 AW (Sigma-Aldrich). At ≥5min post inoculation the plants were lightly misted with tap water to remove residual abrasive, covered with clear plastic bags or propagator lids and incubated overnight at no or very low light, following which plants were returned to standard growth conditions. Systemically infected leaves showing moderate mosaic symptoms where collected at 14-21 dpi and used as a source of inoculum for rub-inoculation of new batches of wheat plants. This passaging sequence was repeated seven times.

Small RNA sequencing (small RNA-seq)

Systemic leaves of three cv. Riband and three cv. Chinese Spring FoMV-infected wheat plants were collected at 26 days after the seventh passaging and pooled. Total RNA was extracted using TRIzol (Invitrogen) following the manufacturer's instructions with the exception that the chloroform extraction was repeated once. Total RNA was treated with DNase I (Promega) at 1U per µg of RNA for 35 min at 37°C, and then purified by extraction with phenol:chloroform and then with chloroform, followed by standard precipitation with ethanol. RNA pellets were re-suspended in nuclease-free water (Promega) and RNA quality was assessed using a 2100 Bioanalyser (Agilent Technologies). Total RNA samples from two independent pools of leaves were used for small RNA-seq on an Illumina HiSeq 2500 (1x50 bp) platform at Fasteris (Plan-les-Ouates, Switzerland).

Assembly of small RNA-seq reads to obtain a consensus master genome of FoMV isolate PV139

The adapter trimmed small RNA reads in the range between 20-24 nt were assembled *de novo* into contigs using Velvet (v1.2.09) (Zerbino, 2010) with the best *k*-mer value of 19, and using SOAPdenovo2 (v2.04) (Luo et al., 2012) with a multi *k*-mer setting of 19-24. The resulting assemblies were aligned using Lastz (v1.02.00) (Harris, 2007) with a publicly available FoMV genomic RNA sequence (GenBank accession EF630359.1) to orientate the *de novo* assembly contigs and create a *de novo* assembly consensus sequence. The small RNA reads were then mapped back to the assemblies using Bowtie2 (v2.2.0) (Langmead and Salzberg, 2012) using default settings with end to end mapping algorithm in a cyclical method of improvement, to check for concordance and to correct any erroneous small INDELs (INsertion/DELetion) and SNPs (single nucleotide polymorphisms) from the *de novo* assemblies.

Construction of an infectious full-length cDNA clone of the FoMV isolate pCF RNA genome

All PCRs described below were done using the high-fidelity DNA polymerases Phusion (New England Biolabs) or Platinum SuperFi (Invitrogen) unless otherwise stated, and all the constructs were verified by Sanger sequencing.

The genome of FoMV isolate pCF was cloned from a previously available cDNA clone called pCF into a binary vector as follows. CaMV 35S promoter sequence was amplified by PCR from the vector pGR106 (Lu et al., 2003) with the oligonucleotides 5'35Sp and 5'FoMV-3'35Sp (Table S4). The 5'-part of FoMV isolate pCF was amplified by PCR from the plasmid pCF with the oligonucleotides 3'35Sp-5'FoMV and SpeI-FoMV1040R (Table S4). The two resulting amplicons were fused by PCR with the oligonucleotides 5'35Sp and SpeI-FoMV1040R, using a 38-nt long complementary region which was artificially introduced at the 3'-extremity of 35S promoter and at the 5'-extremity of FoMV amplicons.

545   The resulting 35S-5'-FoMV fragment was then cloned between *Eco*RV *Spe*I recognition sites into
546   *Eco*RV and *Spe*I-digested pGR106 vector backbone to produce the plasmid pGR-5'-pCF. Finally, the
547   3'-part of FoMV pCF was obtained by *Blp*I and *Xba*I digestion of pCF plasmid and this fragment was
548   then inserted into the *Blp*I and *Spe*I-digested pGR-5'-pCF. The resulting construct was named pGR-
549   FoMV.pCF. In this binary plasmid, the FoMV genome is under control of CaMV 35S promoter, and is
550   flanked at the 3'-end by the *A. tumefaciens* nopaline synthase gene (*nos*) terminator sequence.

551

Construction of first generation FoMV VOX vectors based on the isolate pCF

553   First, a general cloning plasmid pMA-RQ (Thermo Fisher Scientific) was modified by introducing *Spe*I
554   and *Xho*I restriction sites into the multiple cloning site, creating a plasmid pBxs. This was done using
555   oligonucleotide-directed mutagenesis on the whole plasmid (Silva et al., 2017) and primers pBxs-fw
556   and pBxs-rev. FoMV cDNA clone pCF was then digested with *Spe*I plus *Xho*I and a fragment
557   corresponding to the 1,627-nt long 3'-most portion of the FoMV genome, including a 65-nt long
558   poly(A) tail, was cloned into *Spe*I plus *Xho*I-digested pBxs generating a plasmid pB-F. Then, a
559   multiple cloning site (MCS) containing sites for digestion with the restriction enzymes *Sal*I, *Cla*I, *Asc*I,
560   *Hpa*I and *Xba*I was inserted into pB-F immediately upstream of the predicted FoMV CP sgp (sgp2) by
561   oligonucleotide-directed mutagenesis using two consecutive PCR cycles and primers pB-Fmcs-10-
562   fw1 and pB-Fmcs-10-rev1 for the first reaction, and pB-Fmcs-10-fw2 and pB-Fmcs-10-rev2 for the
563   second reaction. The resulting plasmid, pBFmcs-10, was digested with *Sph*I and *Asc*I and ligated with
564   a gene synthesized DNA fragment (Invitrogen), digested with the same two enzymes, comprising a
565   101-bp sequence of the predicted FoMV sgp2 (nucleotides 5280-5380 in FoMV pCF) and a
566   downstream MCS containing restriction sites for *Sal*I, *Cla*I, *Asc*I, *Hpa*I and *Xba*I, generating a plasmid
567   pB-Fsgp2-101/pCF. Three other predicted FoMV sgp2 sequences of 90, 55 and 45 nts (90-bp
568   sequence: nucleotides 5291-5380 in FoMV pCF; 55-bp sequence: nucleotides 5291-5345; 45-bp
569   sequence: nucleotides 5291-5324) in size were produced by gene synthesis upstream of the above-
570   mentioned MCS, digested with *Sph*I and *Asc*I and ligated into a *Sph*I plus *Asc*I-digested pBF-mcs
571   plasmid produced by oligonucleotide-directed mutagenesis on the plasmid pBF using two consecutive
572   PCR cycles and primers pB-Fmcs-fw1 and pB-Fmcs-rev1 for the first reaction, and pB-Fmcs-fw2 and
573   pB-Fmcs-rev2 for the second reaction. The corresponding plasmids were named pB-Fsgp2-90/pCF,
574   pB-Fsgp2-55/pCF and pB-Fsgp2-45/pCF, respectively.

575   The coding sequence of the S65T variant of GFP gene (Heim et al., 1995) was amplified from the
576   plasmid pActIsGFP using the oligonucleotides GFP5'-ClaI-fw and GFP3'-XbaI-rev. The corresponding
577   amplicon was digested with *Cla*I plus *Xba*I and cloned into *Cla*I plus *Xba*I-digested pB-Fsgp2-
578   101/pCF, pB-Fsgp2-90/pCF, pB-Fsgp2-55/pCF and pB-Fsgp2-45/pCF. The generated plasmids were
579   named pB-Fsgp2-101/pCF-GFP, pB-Fsgp2-90/pCF-GFP, pB-Fsgp2-55/pCF-GFP and pB-Fsgp2-
580   45/pCF-GFP. The empty and the GFP-containing pB-Fsgp2-/pCF plasmids were digested by *Spe*I
581   and *Xho*I and inserted into *Spe*I plus *Xho*I digested pGR.FoMV.pCF. The obtained empty VOX
582   vectors were named pCF101, pCF90, pCF55 and pCF45 whereas their GFP-containing counterparts
583   were named pCF101-GFP, pCF90-GFP, pCF55-GFP and pCF45-GFP respectively.

584   FoMV pCF derived expression constructs have been inoculated onto plants and analyzed as specified
585   in the sections below and summarized in Table S5.

586

Construction of an infectious full-length cDNA clone of the FoMV isolate PV139 RNA genome

588   Commercially synthesized (Invitrogen) full-length cDNA copy of the FoMV isolate PV139 was cloned
589   into the pGR106 vector backbone between *Eco*RV and *Afl*II restriction nuclease sites generating the
590   binary plasmid pGR-FoMV.PV139. A full-length FoMV cDNA in this plasmid is flanked at the 5'-end by
591   the CaMV 35S promoter and at the 3'-end by the *nos* terminator sequence.

592

Construction of the FoMV VOX vectors PV101 and PV101gw

594   The FoMV isolate PV139-derived expression vector PV101 enabling integration of genes of interest
595   using a standard restriction-enzyme cloning was constructed as follows. A fragment of pB-
596   Fsgp2/pCF-101 was amplified by PCR (PCR1) with primers PV101-F2 and PV101-R2. A second PCR
597   (PCR2) was done using the vector pGR-FoMV.PV139 as the template and primers PV101-F3 and
598   PVsorg-8R. A fusion PCR (PCR3) was then carried out using a 1:1 mixture of amplicons produced in

599   PCR1 and PCR2 as the template and primers PV101-F2 and PVsorg-8R. Finally, a fourth PCR
600   (PCR4) was performed using the vector pGR-FoMV.PV139 as the template and primers PVsorg-6F
601   and PV101-R1. Amplicons produced in PCR3 and PCR4 were then assembled into *Spe*I plus *Avr*II-
602   digested plasmid pGR-FoMV.PV139 using the NEBuilder HiFi DNA assembly system (New England
603   Biolabs) following the manufacturer protocol to obtain the vector PV101.

604   A Gateway compatible FoMV VOX vector was created as follows. A first PCR (PCR1) was done using
605   pGR-FoMV.PV139 as the template and the oligonucleotides PVsorg-6F and PV101gw-R1. A
606   Gateway cassette was amplified by PCR (PCR2) from the vector pGWB605 (Nakamura et al., 2010)
607   using the oligonucleotides PV101gw-F2' and PV101gw-R2'. A third amplicon (PCR3) was produced
608   from pGR-FoMV.PV139 with the oligonucleotides PV101gw-F3 and PVsorg-8R. Amplicons from
609   PCR1, PCR2 and PCR3 were assembled into *Spe*I plus *Avr*II digested pGR-FoMV.PV139 using the
610   NEBuilder HiFi DNA assembly system to obtain the vector PV101gw.

611

Cloning of genes encoding reporter proteins and a fungal necrotrophic effector protein into the FoMV isolate PV139-derived expression vectors

614   The coding sequence of the S65T variant of *GFP* gene was amplified from the plasmid pActIsGFP
615   using the oligonucleotides GFP5'-ClaI-fw and GFP3'-XbaI-rev. The corresponding amplicon was
616   digested with *Cla*I plus *Xba*I and cloned into *Cla*I plus *Xba*I-digested PV101 to create PV101-GFP.
617   The *GFP* coding sequence was also amplified from pActIsGFP using the oligonucleotides attB1-GFP-
618   F and attB2-GFP-R, and the obtained amplicon was recombined into the Gateway enabled FoMV
619   vector PV101gw using BP clonase II enzyme mix (Invitrogen) following the manufacturer protocol, to
620   produce PV101gw-GFP.

621   The coding sequence of the *P. nodorum ToxA* gene was amplified from the plasmid pDONR207-
622   ToxA+SP-STOP using the oligonucleotides ClaI-ToxA-F and XbaI-ToxA-R. The amplicon was then
623   digested using *Cla*I plus *Xba*I and cloned into *Cla*I plus *Xba*I-digested PV101 to produce PV101-
624   ToxA.

625   The coding sequence of GUSPlus (Broothaerts et al., 2005) in the plasmid pRRes104.293 served as
626   a template for two PCRs producing partially overlapping amplicons using primers ClaI-woGUS-F1 and
627   woGUS-R1 (PCR 1) and woGUS-F2 and XbaI-woGUS-R2 (PCR 2). The amplicons from PCR1 and
628   PCR2 were then fused together using an additional cycle of PCR and the oligonucleotides ClaI-
629   woGUS-F1 and XbaI-woGUS-R2. The resulting amplicon, containing a GUSPlus coding sequence
630   with the internal *Cla*I recognition site removed, was digested using *Cla*I and *Xba*I and cloned into *Cla*I
631   plus *Xba*I-digested PV101 to obtain PV101-GUSPlus.

632   FoMV PV139 derived expression constructs have been inoculated onto plants and analyzed as
633   specified in the sections below and summarized in Table S5.

634

Inoculation of *N. benthamiana*, wheat and maize seedlings with the FoMV expression constructs

637   FoMV PV101, PV101gw and other expression constructs derived from these binary vectors and the
638   plasmid pBIN61-p19 for expression of a well-known RNA silencing suppressor protein p19 from
639   *Tomato bushy stunt virus* (TBSV), were introduced into the *A. tumefaciens* strain GV3101 pCH32
640   pSa-Rep (Hellens et al., 2000) by electroporation. Bacterial cultures were obtained by inoculating
641   single colonies in liquid Luria-Bertani medium supplemented with gentamycin (25 µg mL^{-1}) and
642   kanamycin (50 µg mL^{-1}) followed by incubation at 28°C for 20 h under constant shaking (250 rpm).
643   Agrobacterium cells were pelleted at 2,013 *g* for 20 min at 17 °C and then re-suspended in an
644   infiltration medium containing 10 mM MES pH5.6, 10 mM MgCl$_2$ and 100 µM acetosyringone.
645   Bacterial suspensions were adjusted to an OD$_{600}$ 1.2-1.5 and incubated at room temperature for ≥3 h.
646   To initiate infection in *N. benthamiana* plants, each FoMV vector-containing Agrobacterium
647   suspension was mixed with an equal volume of pBIN61-P19-containing Agrobacterium suspension
648   and then pressure infiltrated into the abaxial side of fully expanded leaves of young, 6-8 leaf-stage,
649   seedlings using a needleless syringe.

650   To initiate infection in wheat and maize plants, leaves of young seedlings were rub-inoculated using a
651   FoMV-containing sap prepared from *N. benthamiana* leaves agroinfiltrated as described above and
652   harvested at 5-7 days post-infiltration. The sap, produced by finely grinding *N. benthamiana* leaves in

653 0.67 w/v deionized water using mortar and pestle, was supplemented with 1 % (w/v) Celite 545 AW
654 (Sigma-Aldrich) and used for rub-inoculation of the first two leaves of 2-leaf stage wheat seedlings or
655 the first three leaves of 3-4-leaf stage maize seedlings. At ≥5 min post inoculation leaves were
656 sprayed with the tap water to remove the residual sap and Celite, plants bagged and kept under high
657 humidity and low light for ~ 24 h before returned to the standard growth conditions.

658

Reverse transcription PCR (RT-PCR)

660 Total RNA was extracted from FoMV- or mock-inoculated or -agroinfiltrated plants using TRIzol
661 (Invitrogen), and then treated with RQ1 RNase-free DNase (Promega) following the manufacturer's
662 instructions. First-strand cDNAs were produced using SuperScript III Reverse Transcriptase
663 (Invitrogen) and random hexamer primers following the manufacturer's protocol and used as
664 templates for PCR with the GoTaq G2 DNA Polymerase (Promega). For detection of FoMV the
665 oligonucleotides qFoMV3464F and qFoMV3597R spanning nucleotides 3464 – 3597 in ORF1 were
666 used. The housekeeping internal control *N. benthamiana* gene *PP2A* and wheat gene *CDC48*
667 (Paolacci et al., 2009) were detected by PCR using the oligonucleotides NbPP2AF-NbPP2A (Liu et
668 al., 2012) and TaCDC48F-TaCDC48R (Lee et al., 2014), respectively.

669

Immuno-detection of GFP and FoMV coat protein (CP)

671 Aliquots of 50-100 mg of leaf samples were ground in 1.5-mL tubes with 6 v/w suspension buffer (100
672 mM Tris-HCl, pH 8, 1 mM DL-Dithiothreitol) using micro-pestles and centrifuged at 16,100 *g* for 1 min
673 to pellet any cell debris. One hundred μL of leaf extract were supplemented with 33 μL 4X Laemmli
674 extraction buffer (8% SDS, 20% 2-mercaptoethanol, 40% glycerol, 0.008% bromophenol blue, 0.25 M
675 Tris-HCl pH 6.8) and incubated at 95°C for 5 min to allow denaturation of proteins. The samples were
676 loaded onto a 16 % SDS-polyacrylamide gel. Proteins were separated by electrophoresis in 25 mM
677 Tris, 192 mM glycine, 0.1% (v/v) SDS and then electro transferred to a nitrocellulose membrane
678 Protran Premium 0.45 NC (GE Healthcare Life Sciences) for 90 min at 90 V in 25 mM Tris, 192 mM
679 glycine, 20% (v/v) methanol. After transfer, the membranes were stained by incubating in a Ponceau
680 S (Sigma-Aldrich) solution (5% acetic acid (v/v), 0.1% Ponceau S (w/v)) for 5 min to verify that equal
681 total protein was loaded for each sample. The membranes were then destained by rinsing in PBS-T
682 buffer (50 mM Tris, 150 mM NaCl and 0.1% (v/v) Tween 20) and then blocked in PBS-T
683 supplemented with 5% (w/v) dry milk for 45 min at room temperature and under constant shaking (70
684 RPM). Blocked membranes were incubated overnight at 4°C under constant shaking with primary
685 antibodies diluted in PBS-T supplemented with 5% dry milk. The rabbit anti-GFP tag monoclonal
686 antibody (ref G10362, Invitrogen) used in Figure 2 was diluted at 1:200. The anti-GFP polyclonal
687 antibody (ref A-11122, Invitrogen) used in Figure 6 and Figure S5 was diluted at 1:2000 and the rabbit
688 anti FoMV-CP polyclonal antibody (ChinaPeptides Co. Ltd., Shanghai, China) was diluted at 1:5000.
689 Non-bound antibodies were eliminated by rinsing the membranes three times in PBS-T for 15 min at
690 room temperature under constant shaking. Incubation with secondary antibody (goat anti-rabbit-
691 peroxidase antibody, ref A0545, Sigma-Aldrich) diluted at 1:10000 in PBS-T plus 5% dry milk was
692 performed for 3 hours at room temperature under constant shaking. Non-bound antibodies were
693 removed by rinsing the membranes three times in PBS-T for 10 min at room temperature under
694 constant shaking. Membrane-bound immune complexes were revealed with ECL Prime kit (GE
695 Healthcare Life Sciences). Chemiluminescence signals were visualized using Hyperfilm ECL (GE
696 Healthcare Life Sciences).

697

GUS staining

699 Leaf segments were placed into 6-well plates (Thermo Fisher Scientific) and immersed in staining
700 solution (57 mM sodium phosphate dibasic, 42 mM sodium phosphate monobasic, 10 mM EDTA,
701 0.01% Triton X-100 (v/v), 1 mM potassium ferricyanide, 1mM potassium ferrocyanide, 0.5 mg mL^{-1} 5-
702 bromo-4-chloro-3-indolyl-beta-D-glucuronic acid (X-GLUC) (Thermo Fisher Scientific)). The samples
703 were then vacuum-infiltrated several times for 10 min to help the staining solution penetrate leaves.
704 The plates were sealed with cling film and incubated in the dark at 37°C for up to 24 hours. The
705 staining solution was removed and the samples were de-stained in 70% ethanol at room temperature
706 and under constant agitation. Ethanol was changed every 24-48 h until completion of the de-staining

707   process. Samples were illuminated using a white light box (Edvotek, Washington, DC, USA) for
708   photography with a Nikon D90 camera.

709

Stereomicroscopy

711   Plant samples were observed with a Leica M205 FA stereomicroscope (Leica Microsystems Ltd).
712   Fluorescence was visualized using either a GFP2 (excitation filter: 460-500 nm; longpass filter 510
713   nm) or a GFP3 filter set (excitation filter: 450-490 nm; bandpass filter 500-550 nm). Pictures were
714   taken using Leica LAS AF software (Leica Microsystems Ltd).

715

Photography

717   Full leaf photographs were taken using a Nikon D90 (*N. benthamiana* and wheat) or an Olympus OM-
718   D E-M1 Mark II camera (maize). For the fluorescence photography, plants were illuminated with the
719   blue light (440-460 nm excitation) using a Dual Fluorescent Protein flashlight (Nightsea, Lexington,
720   MA, USA). Longpass (510 nm) or bandpass (500-555 nm) filters (Midwest Optical Systems, Palatine,
721   IL, USA) were mounted onto the camera objectives to block blue or blue plus red light, respectively,
722   reflected from the excitation source. Maize full leaf fluorescence photographs were taken using the
723   Live Composite Time mode of the Olympus OM-D E-M1 Mark II camera.

724

Accession Numbers

726   Raw next generation small RNA sequencing data have been deposited to the European Nucleotide
727   Archive under the accession number PRJEB21979. The complete sequences of FoMV pCF and
728   PV139 were submitted to GenBank under accession numbers MF573298 and MF573299,
729   respectively.

730

731

SUPPLEMENTAL DATA

733   **Figure S1.** Sequences of the four differently sized sgp2 duplications used for development of a series
734   of FoMV vectors.

735   **Figure S2.** Progression of PV101-mediated GFP expression over time in the directly inoculated wheat
736   leaves.

737   **Figure S3.** Assessment of PV101-mediated GFP expression in systemically infected wheat and
738   maize leaves.

739   **Figure S4.** Gateway-enabled FoMV vector PV101gw-mediated expression of green fluorescent
740   protein (GFP) in *Nicotiana benthamiana*.

741   **Figure S5.** Comparison of protein expression efficiency from FoMV vectors PV101 and PV169.

742   **Table S1.** Single nucleotide polymorphisms (SNPs) identified between genomes of FoMV pCF and
743   FoMV PV139.

744   **Table S2.** Assessment of PV101-mediated GFP expression in wheat cultivars of diverse geographical
745   origin.

746   **Table S3.** FoMV-directed expression of GUSPlus in maize line B73.

747   **Table S4.** Oligonucleotides used in this study.

748   **Table S5.** Summary of the experiments involving FoMV expression vectors carried out in this study.
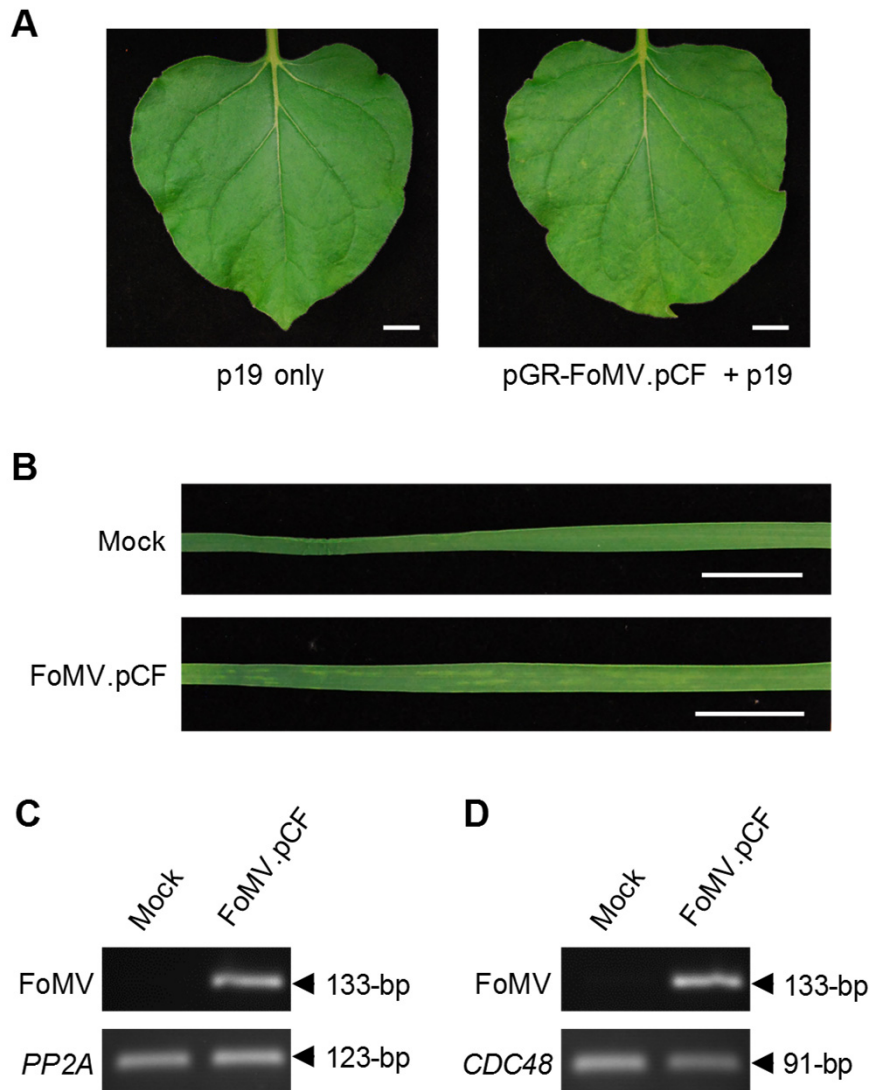
749

750

772

773

774   **LITERATURE CITED**

775   **Broothaerts W, Mitchell HJ, Weir B, Kaines S, Smith LMA, Yang W, Mayer JE, Roa-Rodríguez C,**
776   **Jefferson RA** (2005) Gene transfer to plants by diverse species of bacteria. Nature **433:** 629-633
777   **Brown RH, Hattersley PW** (1989) Leaf anatomy of C_3-C_4 species as related to evolution of C_4
778   photosynthesis. Plant Physiol **91:** 1543-1550
779   **Chapman S, Kavanagh T, Baulcombe D** (1992) *Potato virus X* as a vector for gene expression in
780   plants. Plant J **2:** 549-557
781   **Choi IR, Stenger DC, Morris TJ, French R** (2000) A plant virus vector for systemic expression of
782   foreign genes in cereals. Plant J **23:** 547-555
783   **Csorba T, Burgyán J** (2016) Antiviral silencing and suppression of gene silencing in plants. *In* A Wang,
784   X Zhou, eds, Current Research Topics in Plant Virology. Springer International Publishing, Cham,
785   pp 1-33
786   **Dagvadorj B, Ozketen AC, Andac A, Duggan C, Bozkurt TO, Akkaya MS** (2017) A *Puccinia*
787   *striiformis* f. sp. *tritici* secreted protein activates plant immunity at the cell surface. Sci Rep **7:** 1141
788   **Dickmeis C, Fischer R, Commandeur U** (2014) *Potato virus X*-based expression vectors are stabilized
789   for long-term production of proteins and larger inserts. Biotechnol J **9:** 1369-1379
790   **Domingo E, Sheldon J, Perales C** (2012) Viral quasispecies evolution. Microbiol Mol Biol Rev **76:**
791   159-216
792   **Faris JD, Zhang Z, Lu H, Lu S, Reddy L, Cloutier S, Fellers JP, Meinhardt SW, Rasmussen JB,**
793   **Xu SS, Oliver RP, Simons KJ, Friesen TL** (2010) A unique wheat disease resistance-like gene
794   governs effector-triggered susceptibility to necrotrophic pathogens. Proc Natl Acad Sci USA **107:**
795   13544-13549
796   **Franco-Orozco B, Berepiki A, Ruiz O, Gamble L, Griffe LL, Wang S, Birch PRJ, Kanyuka K,**
797   **Avrova A** (2017) A new proteinaceous pathogen-associated molecular pattern (PAMP) identified in
798   Ascomycete fungi induces cell death in Solanaceae. New Phytol **214:** 1657-1672
799   **Friesen TL, Stukenbrock EH, Liu ZH, Meinhardt S, Ling H, Faris JD, Rasmussen JB, Solomon**
800   **PS, McDonald BA, Oliver RP** (2006) Emergence of a new disease as a result of interspecific
801   virulence gene transfer. Nat Gen **38:** 953-956
802   **Hamilton CM** (1997) A binary-BAC system for plant transformation with high-molecular-weight DNA.
803   Gene **200:** 107-116
804   **Harris RS** (2007) Improved Pairwise Alignment of Genomic DNA. PhD Thesis, The Pennsylvania State
805   University
806   **Heim R, Cubitt AB, Tsien RY** (1995) Improved green fluorescence. Nature **373:** 663-664
807   **Hellens RP, Edwards EA, Leyland NR, Bean S, Mullineaux PM** (2000) pGreen: a versatile and
808   flexible binary Ti vector for Agrobacterium-mediated plant transformation. Plant Mol Biol **42:** 819-
809   832

810 **Ji Q, Yang B, Lee M, Chen Y, Lubberstedt T** (2010) Mapping of quantitative trait loci/locus conferring
811   resistance to *Foxtail mosaic virus* in maize using the intermated B73 x Mo17 population. Plant Breed
812   **129:** 721-723
813 **Kettles GJ, Bayon C, Canning G, Rudd JJ, Kanyuka K** (2017) Apoplastic recognition of multiple
814   candidate effectors from the wheat pathogen *Zymoseptoria tritici* in the nonhost plant *Nicotiana*
815   *benthamiana*. New Phytol **213:** 338-350
816 **Kettles GJ, Bayon C, Sparks C, Canning G, Kanyuka K, Rudd JJ** (2017) Characterisation of an
817   antimicrobial and phytotoxic ribonuclease secreted by the fungal wheat pathogen *Zymoseptoria*
818   *tritici*. New Phytol **217**: 320-331
819 **Kreuze J** (2014) siRNA Deep Sequencing and Assembly: Piecing Together Viral Infections. *In* ML
820   Gullino, PJM Bonants, eds, Detection and Diagnostics of Plant Pathogens. Springer Netherlands,
821   Dordrecht, pp 21-38
822 **Lacomme C, Santa Cruz S** (1999) Bax-induced cell death in tobacco is similar to the hypersensitive
823   response. Proc Natl Acad Sci USA **96:** 7956-7961
824 **Langmead B, Salzberg SL** (2012) Fast gapped-read alignment with Bowtie 2. Nat Methods **9:** 357-
825   359
826 **Lee WS, Hammond-Kosack KE, Kanyuka K** (2012) *Barley stripe mosaic virus*-mediated tools for
827   investigating gene function in cereal plants and their pathogens: Virus-induced gene silencing, Host-
828   mediated gene silencing, and Virus-mediated overexpression of heterologous protein. Plant Physiol
829   **160:** 582-590
830 **Lee WS, Rudd JJ, Hammond-Kosack KE, Kanyuka K** (2014) *Mycosphaerella graminicola* LysM
831   effector-mediated stealth pathogenesis subverts recognition through both CERK1 and CEBiP
832   homologues in wheat. Mol Plant Microbe Interact **27:** 236-243
833 **Lin MK, Chang BY, Liao JT, Lin NS, Hsu YH** (2004) Arg-16 and Arg-21 in the N-terminal region of the
834   triple-gene-block protein 1 of *Bamboo mosaic virus* are essential for virus movement. J Gen Virol
835   **85:** 251-259
836 **Liu D, Shi L, Han C, Yu J, Li D, Zhang Y** (2012) Validation of reference genes for gene expression
837   studies in virus-infected *Nicotiana benthamiana* using quantitative real-time PCR. PLoS One **7:**
838   e46451
839 **Liu N, Xie K, Jia Q, Zhao JP, Chen TY, Li HG, Wei X, Diao XM, Hong YG, Liu YL** (2016) *Foxtail*
840   *mosaic virus*-induced gene silencing in monocot plants. Plant Physiol **171:** 1801-1807
841 **Liu Z, Friesen TL, Ling H, Meinhardt SW, Oliver RP, Rasmussen JB, Faris JD** (2006) The Tsn1-
842   ToxA interaction in the wheat-*Stagonospora nodorum* pathosystem parallels that of the wheat-tan
843   spot system. Genome **49:** 1265-1273
844 **Liu Z, Kearney CM** (2010) An efficient *Foxtail mosaic virus* vector system with reduced environmental
845   risk. BMC Biotechnol **10:** 88
846 **Lu R, Malcuit I, Moffett P, Ruiz MT, Peart J, Wu AJ, Rathjen JP, Bendahmane A, Day L, Baulcombe**
847   **DC** (2003) High throughput virus-induced gene silencing implicates heat shock protein 90 in plant
848   disease resistance. EMBO J **22:** 5690-5699
849 **Luo RB, Liu BH, Xie YL, Li ZY, Huang WH, Yuan JY, He GZ, Chen YX, Pan Q, Liu YJ, Tang JB,**
850   **Wu GX, Zhang H, Shi YJ, Liu Y, Yu C, Wang B, Lu Y, Han CL, Cheung DW, Yiu SM, Peng SL,**
851   **Zhu XQ, Liu GM, Liao XK, Li YR, Yang HM, Wang J, Lam TW, Wang J** (2012) SOAPdenovo2: an
852   empirically improved memory-efficient short-read *de novo* assembler. Gigascience **1:** 6
853 **Majer E, Llorente B, Rodriguez-Concepcion M, Daros JA** (2017) Rewiring carotenoid biosynthesis
854   in plants using a viral vector. Sci Rep **7:** 10
855 **Manning VA, Chu AL, Scofield SR, Ciuffetti LM** (2010) Intracellular expression of a host-selective
856   toxin, ToxA, in diverse plants phenocopies silencing of a ToxA-interacting protein, ToxABP1. New
857   Phytol **187:** 1034-1047
858 **Manning VA, Ciuffetti LM** (2005) Localization of Ptr ToxA produced by *Pyrenophora tritici-repentis*
859   reveals protein import into wheat mesophyll cells. Plant Cell **17:** 3203-3212
860 **Mei Y, Zhang CQ, Kernodle BM, Hill JH, Whitham SA** (2016) A *Foxtail mosaic virus* vector for Virus-
861   induced gene silencing in maize. Plant Physiol **171:** 760-772
862 **Meng Y, Moscou MJ, Wise RP** (2009) Blufensin1 negatively impacts basal defense in response to
863   barley powdery mildew. Plant Physiol **149:** 271-285
864 **Nakamura S, Mano S, Tanaka Y, Ohnishi M, Nakamori C, Araki M, Niwa T, Nishimura M, Kaminaka**
865   **H, Nakagawa T, Sato Y, Ishiguro S** (2010) Gateway binary vectors with the bialaphos resistance
866   gene, *bar*, as a selection marker for plant transformation. Biosci Biotechnol Biochem **74:** 1315-1319
867 **Panwar V, McCallum B, Bakkeren G** (2013) Endogenous silencing of *Puccinia triticina* pathogenicity
868   genes through in planta-expressed sequences leads to the suppression of rust diseases on wheat.
869   Plant J **73:** 521-532

870 **Paolacci AR, Tanzarella OA, Porceddu E, Ciaffi M** (2009) Identification and validation of reference
871   genes for quantitative RT-PCR normalization in wheat. BMC Mol Biol **10:** 27
872 **Paulsen AQ, Niblett CL** (1977) Purification and properties of *Foxtail mosaic virus*. Phytopathology **67:**
873   1346-1351
874 **Robertson NL, French R, Morris TJ** (2000) The open reading frame 5A of *Foxtail mosaic virus* is
875   expressed in vivo and is dispensable for systemic infection. Arch Virol **145:** 1685-1698
876 **Schnable PS, Ware D, Fulton RS, Stein JC, Wei F, Pasternak S, Liang C, Zhang J, Fulton L,**
877   **Graves TA, Minx P, Reily AD, Courtney L, Kruchowski SS, Tomlinson C, Strong C, Delehaunty**
878   **K, Fronick C, Courtney B, Rock SM, Belter E, Du F, Kim K, Abbott RM, Cotton M, Levy A,**
879   **Marchetto P, Ochoa K, Jackson SM, Gillam B, Chen W, Yan L, Higginbotham J, Cardenas M,**
880   **Waligorski J, Applebaum E, Phelps L, Falcone J, Kanchi K, Thane T, Scimone A, Thane N,**
881   **Henke J, Wang T, Ruppert J, Shah N, Rotter K, Hodges J, Ingenthron E, Cordes M, Kohlberg**
882   **S, Sgro J, Delgado B, Mead K, Chinwalla A, Leonard S, Crouse K, Collura K, Kudrna D, Currie**
883   **J, He R, Angelova A, Rajasekar S, Mueller T, Lomeli R, Scara G, Ko A, Delaney K, Wissotski**
884   **M, Lopez G, Campos D, Braidotti M, Ashley E, Golser W, Kim H, Lee S, Lin J, Dujmic Z, Kim**
885   **W, Talag J, Zuccolo A, Fan C, Sebastian A, Kramer M, Spiegel L, Nascimento L, Zutavern T,**
886   **Miller B, Ambroise C, Muller S, Spooner W, Narechania A, Ren L, Wei S, Kumari S, Faga B,**
887   **Levy MJ, McMahan L, Van Buren P, Vaughn MW, Ying K, Yeh CT, Emrich SJ, Jia Y,**
888   **Kalyanaraman A, Hsia AP, Barbazuk WB, Baucom RS, Brutnell TP, Carpita NC, Chaparro C,**
889   **Chia JM, Deragon JM, Estill JC, Fu Y, Jeddeloh JA, Han Y, Lee H, Li P, Lisch DR, Liu S, Liu Z,**
890   **Nagel DH, McCann MC, SanMiguel P, Myers AM, Nettleton D, Nguyen J, Penning BW, Ponnala**
891   **L, Schneider KL, Schwartz DC, Sharma A, Soderlund C, Springer NM, Sun Q, Wang H,**
892   **Waterman M, Westerman R, Wolfgruber TK, Yang L, Yu Y, Zhang L, Zhou S, Zhu Q, Bennetzen**
893   **JL, Dawe RK, Jiang J, Jiang N, Presting GG, Wessler SR, Aluru S, Martienssen RA, Clifton**
894   **SW, McCombie WR, Wing RA, Wilson RK** (2009) The B73 maize genome: complexity, diversity,
895   and dynamics. Science **326:** 1112-1115
896 **Seguin J, Rajeswaran R, Malpica-Lopez N, Martin RR, Kasschau K, Dolja VV, Otten P, Farinelli**
897   **L, Pooggin MM** (2014) *De novo* reconstruction of consensus master genomes of plant RNA and
898   DNA viruses from siRNAs. PLoS One **9:** 8
899 **Seifers DL, Harvey TL, Haber S, She YM, Chernushevich I, Ens W, Standing KG** (1999) Natural
900   infection of sorghum by *Foxtail mosaic virus* in Kansas. Plant Dis **83:** 905-912
901 **Sempere RN, Gomez P, Truniger V, Aranda MA** (2011) Development of expression vectors based
902   on *Pepino mosaic virus*. Plant Methods **7:** 6
903 **Silva D, Santos G, Barroca M, Collins T** (2017) Inverse PCR for point mutation introduction. Methods
904   Mol Biol **1620:** 87-100
905 **Sztuba-Solińska J, Stollar V, Bujarski JJ** (2011) Subgenomic messenger RNAs: Mastering regulation
906   of (+)-strand RNA virus life cycle. Virology **412:** 245-255
907 **Tang C, Wei J, Han Q, Liu R, Duan X, Fu Y, Huang X, Wang X, Kang Z** (2015) PsANT, the adenine
908   nucleotide translocase of *Puccinia striiformis*, promotes cell death and fungal growth. Sci Rep **5:**
909   11241
910 **Tatineni S, McMechan AJ, Bartels M, Hein GL, Graybosch RA** (2015) *In vitro* transcripts of wild-type
911   and fluorescent protein-tagged *Triticum mosaic virus* (family *Potyviridae*) are biologically active in
912   wheat. Phytopathology **105:** 1496-1505
913 **Tatineni S, McMechan AJ, Hein GL, French R** (2011) Efficient and stable expression of GFP through
914   *Wheat streak mosaic virus*-based vectors in cereal hosts using a range of cleavage sites: Formation
915   of dense fluorescent aggregates for sensitive virus tracking. Virology **410:** 268-281
916 **Xu W, Meng Y, Surana P, Fuerst G, Nettleton D, Wise RP** (2015) The knottin-like Blufensin family
917   regulates genes involved in nuclear import and the secretory pathway in barley-powdery mildew
918   interactions. Front Plant Sci **6:** 409
919 **Yuan C, Li C, Yan L, Jackson AO, Liu Z, Han C, Yu J, Li D** (2011) A high throughput *Barley stripe*
920   *mosaic virus* vector for virus induced gene silencing in monocots and dicots. PLoS One **6:** e26468
921 **Zerbino DR** (2010) Using the Velvet *de novo* assembler for short-read sequencing technologies. Curr
922   Protoc Bioinformatics **Chapter 11:** Unit 11.5
923 **Zhang H, Wang L, Hunter D, Voogd C, Joyce N, Davies K** (2013) A *Narcissus mosaic viral* vector
924   system for protein expression and flavonoid production. Plant Methods **9:** 28
925 **Zhang J, Yu DS, Zhang Y, Liu K, Xu KD, Zhang FL, Wang J, Tan GX, Nie XH, Ji QH, Zhao L, Li**
926   **CW** (2017) Vacuum and co-cultivation Agroinfiltration of (germinated) seeds results in *Tobacco rattle*
927   *virus* (TRV) mediated whole-plant virus-induced gene silencing (VIGS) in wheat and maize. Front
928   Plant Sci **8:** 393

A

p19 only | pGR-FoMV.pCF + p19

B

Mock

FoMV.pCF

C

Mock | FoMV.pCF

FoMV ◄ 133-bp

PP2A ◄ 123-bp

D

Mock | FoMV.pCF
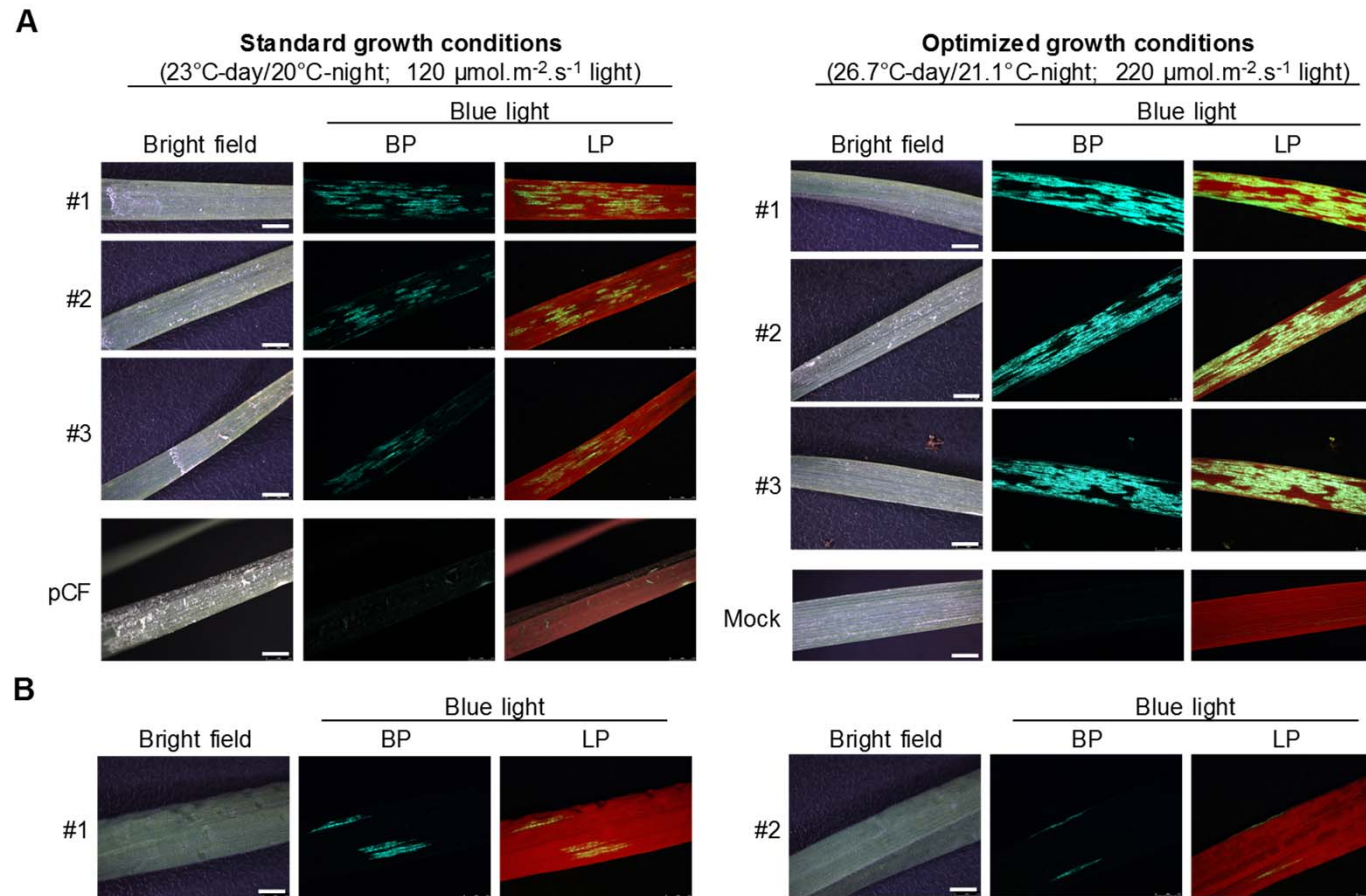
FoMV ◄ 133-bp

CDC48 ◄ 91-bp

Figure 1. Testing infectivity of the first generation FoMV vector pGR-FoMV.pCF in *Nicotiana benthamiana* and wheat. A: Upper uninoculated leaves from mock- or virus-inoculated *N. benthamiana* plants at 19-dpi. Bar = 20 mm. **B:** Upper uninoculated leaves from mock- or virus-inoculated wheat cv. Riband plants at 13-dpi. Bar = 20 mm. **C-D:** Detection of FoMV RNA in upper uninoculated leaves from mock- or virus-inoculated *N. benthamiana* **(C)** and wheat **(D)** plants using RT-PCR. Housekeeping *N. benthamiana PP2A* **(C)** and wheat *CDC48* (**D**) genes were used as loading controls.
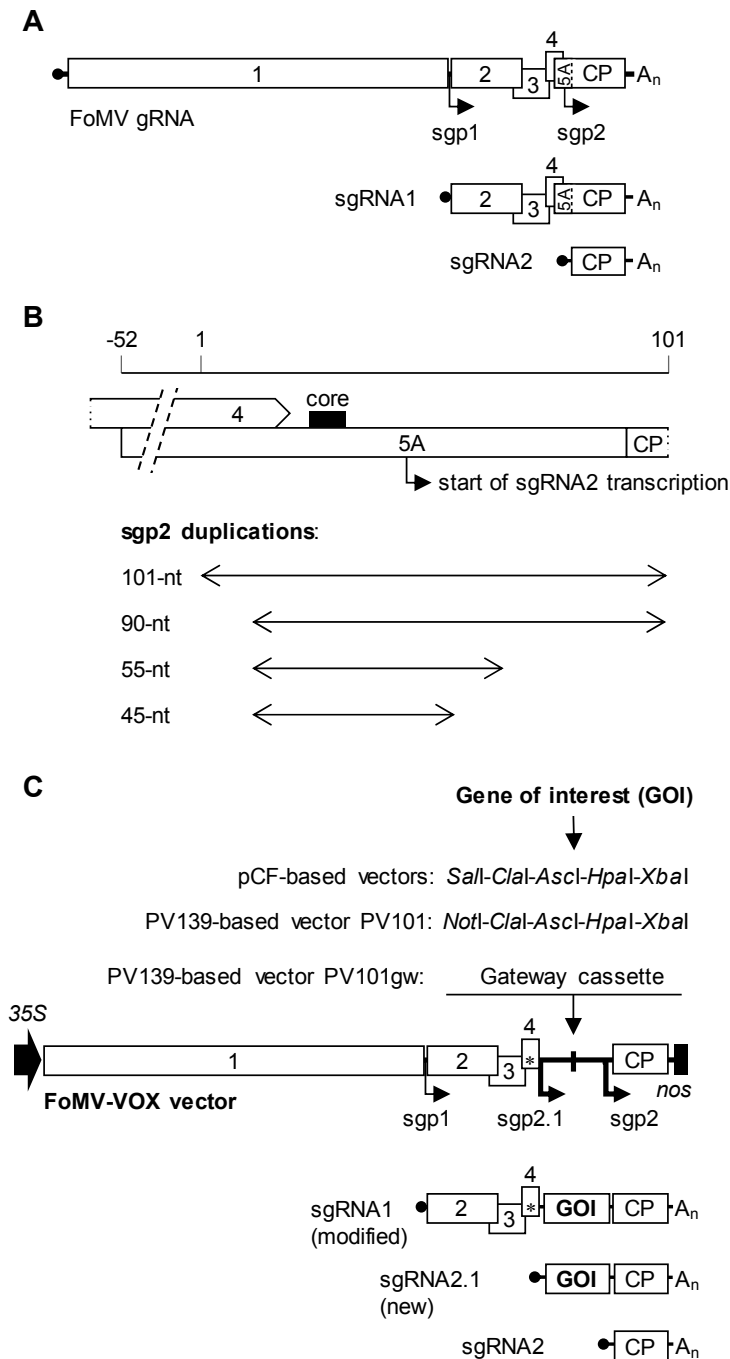
Figure 2. Development of a FoMV expression vector. A: FoMV genome organisation and expression strategy. The viral genomic RNA (gRNA) contains five major open reading frames (ORFs; labelled from 1 to 4, and CP), coding for the polymerase (ORF1), movement proteins (ORF2, 3, 4), and coat protein (CP), and a cryptic ORF5A that gives rise to an N-terminal CP extension with unknown function. ORF1 is expressed from gRNA, whereas ORF2, 3, 4 and CP are expressed from subgenomic (sg) RNA1 and 2, respectively, which are synthesised by the viral polymerase. Synthesis of sgRNAs is driven by subgenomic promoters sgp1 and sgp2. Filled black circle – mRNA cap structure; A_n – poly(A) tail; black arrow – sgRNA transcription start. **B:** A series of FoMV expression vectors were constructed by duplicating differently sized predicted sgp2 sequences, each encompassing a conserved 8-nt core element (**core**). Duplicated sequences were placed downstream of the ORF5A start codon therefore disrupting synthesis of an N-terminal CP extension. **C:** Schematic diagram of the constructed FoMV expression vectors. The gene of interest (**GOI**) in these vectors is inserted between sgp2.1 and sgp2 by restriction enzyme (isolate pCF-based vectors, and PV101 based on the isolate PV139) or Gateway cloning (PV101gw), and expressed from an additional sgRNA2.1 generated from sgp2.1. Spacing between sgp2.1 and sgp2 is drawn not to scale. 35S: CaMV *35S* promoter; *nos*: nopaline synthase terminator; ∗: start codon of ORF5A.
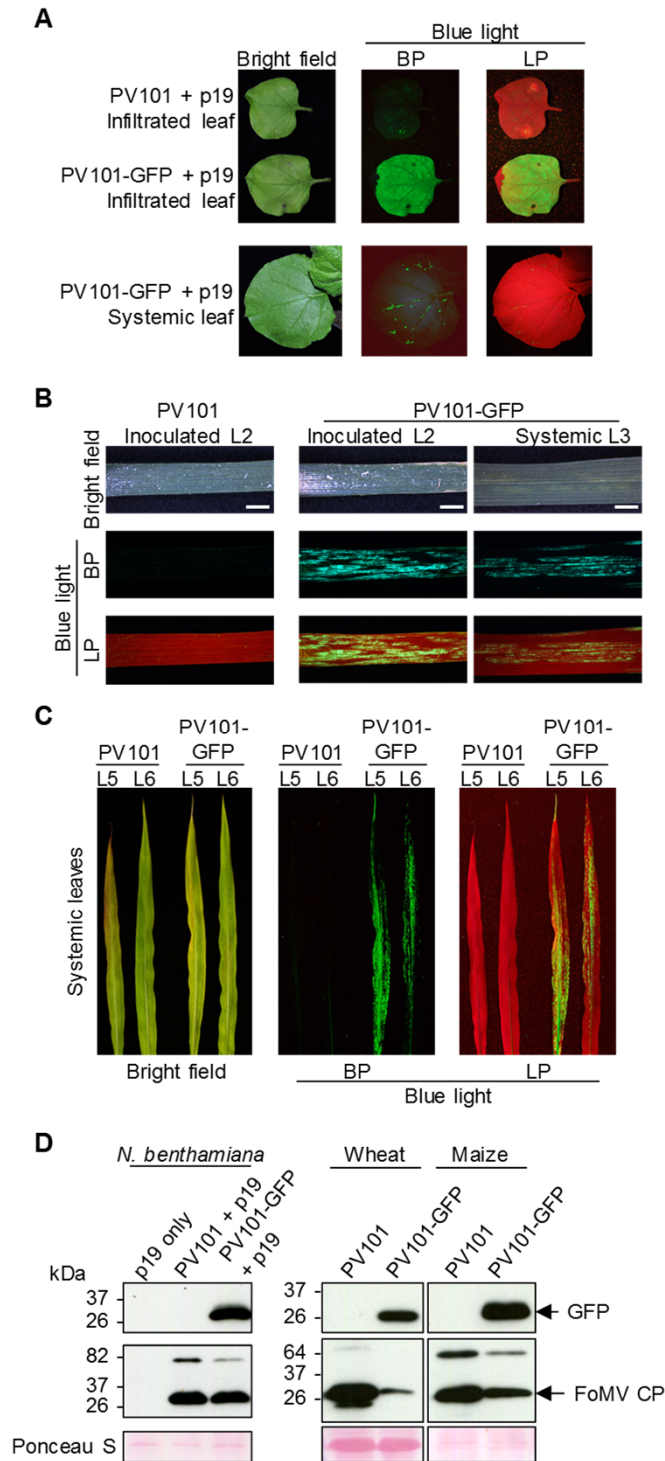
Figure 3. Expression of green fluorescent protein (GFP) from the first generation FoMV VOX vectors in *Nicotiana benthamiana*. A series of four expression vectors generated through duplication of 45-, 55-, 90- and 101-nt sequences spanning the predicted sgp2 sequences were generated based on the full-length infectious FoMV cDNA clone pCF. **A:** *N. benthamiana* leaves co-infiltrated with one of the Agrobacterium strains carrying either an empty vector pCF101 or pCF101-GFP, pCF90-GFP, pCF55-GFP or pCF45-GFP, and an Agrobacterium strain carrying construct for expression of p19 gene silencing suppressor. Representative infiltrated leaves were photographed at 6-dpi with a fluorescence stereomicroscope mounted with bandpass (BP) and longpass (LP) filters, using identical acquisition settings. Bar = 2.5 mm. **B:** Immuno-detection of FoMV CP and GFP in pooled agroinfiltrated leaves from 3 individuals sampled at 3-dpi using the corresponding antibodies. Equal loading was verified by staining the membranes with Ponceau S.

Figure 4. Influence of growth conditions on FoMV-mediated protein expression. **A:** Seedlings of wheat cv. Riband grown under standard or optimized growth conditions were inoculated with pCF101-GFP. Mock-inoculated plants or plants inoculated with the wild-type FoMV pCF served as negative controls. Inoculated leaves (L2) from 3 representative individual plants were photographed at 8-dpi using a fluorescence stereomicroscope mounted with bandpass (BP) and longpass (LP) filters. All fluorescence pictures were taken using identical acquisition settings. Bar = 2.5 mm. **B:** Scant green fluorescent foci observed in the upper uninoculated leaves (L4) of some pCF101-GFP-inoculated plants grown under optimized conditions at 18-dpi.
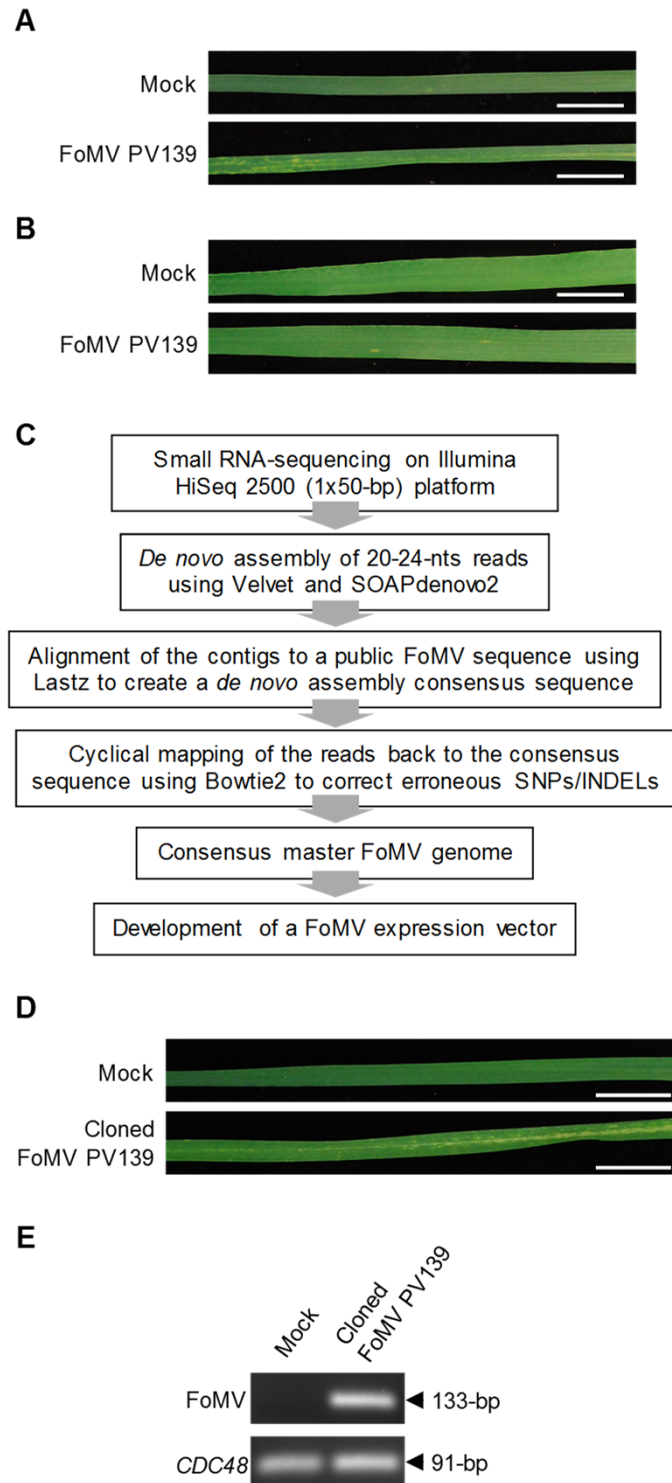
Figure 5. Generation of a full-length infectious cDNA clone of the FoMV isolate PV139.
**A-B:** Symptoms observed on the upper uninoculated leaves of wheat cvs. Riband **(A)** and Bobwhite **(B)** plants infected with the original FoMV PV139 at 21-dpi. No symptoms were observed in mock-inoculated plants. Bar = 20 mm. **C:** Pipeline used to obtain a consensus master genome sequence of FoMV isolate PV139 starting from a small RNA fraction purified from the FoMV-infected leaf material. SNP: single nucleotide polymorphism; INDEL: insertion/deletion polymorphism. **D:** Symptoms observed on the upper uninoculated leaves of wheat cv. Riband plants infected with the full-length infectious FoMV PV139 cDNA clone at 24 dpi. No symptoms were observed in mock-inoculated plants. Bar = 20 mm. **E:** Detection of FoMV RNA in the upper uninoculated leaves of wheat cv. Riband plants infected with the FoMV PV139 cDNA clone by RT-PCR. Wheat *CDC48* was used as a loading control.

Figure 6. Expression of green fluorescent protein (GFP) using the second generation FoMV vector PV101 in plants. A: Directly inoculated (via co-infiltration with Agrobacterium strains carrying PV101-GFP and a construct for expression of p19 gene silencing suppressor) and upper uninoculated leaves of *Nicotiana benthamiana* plants at 7-dpi and 14-dpi, respectively. **B:** Directly inoculated and upper uninoculated (systemic) leaves of wheat cv. Riband at 7-dpi and 14-dpi, respectively. **C:** Systemically infected leaves of maize line B73 plants at 20-dpi. Photos were taken using a camera **(A and C)** or a fluorescence stereomicroscope **(B)** mounted with bandpass (BP) and longpass (LP) filters. Bar = 2.5 mm. **D:** Immuno-detection of GFP and FoMV-CP in pooled systemically infected leaves from 3 individuals of different plant species sampled at 14-dpi using the corresponding antibodies. The presence of fluorescence in PV101-GFP-infected plants was checked before sampling. Equal loading was verified by staining the membranes with Ponceau S.
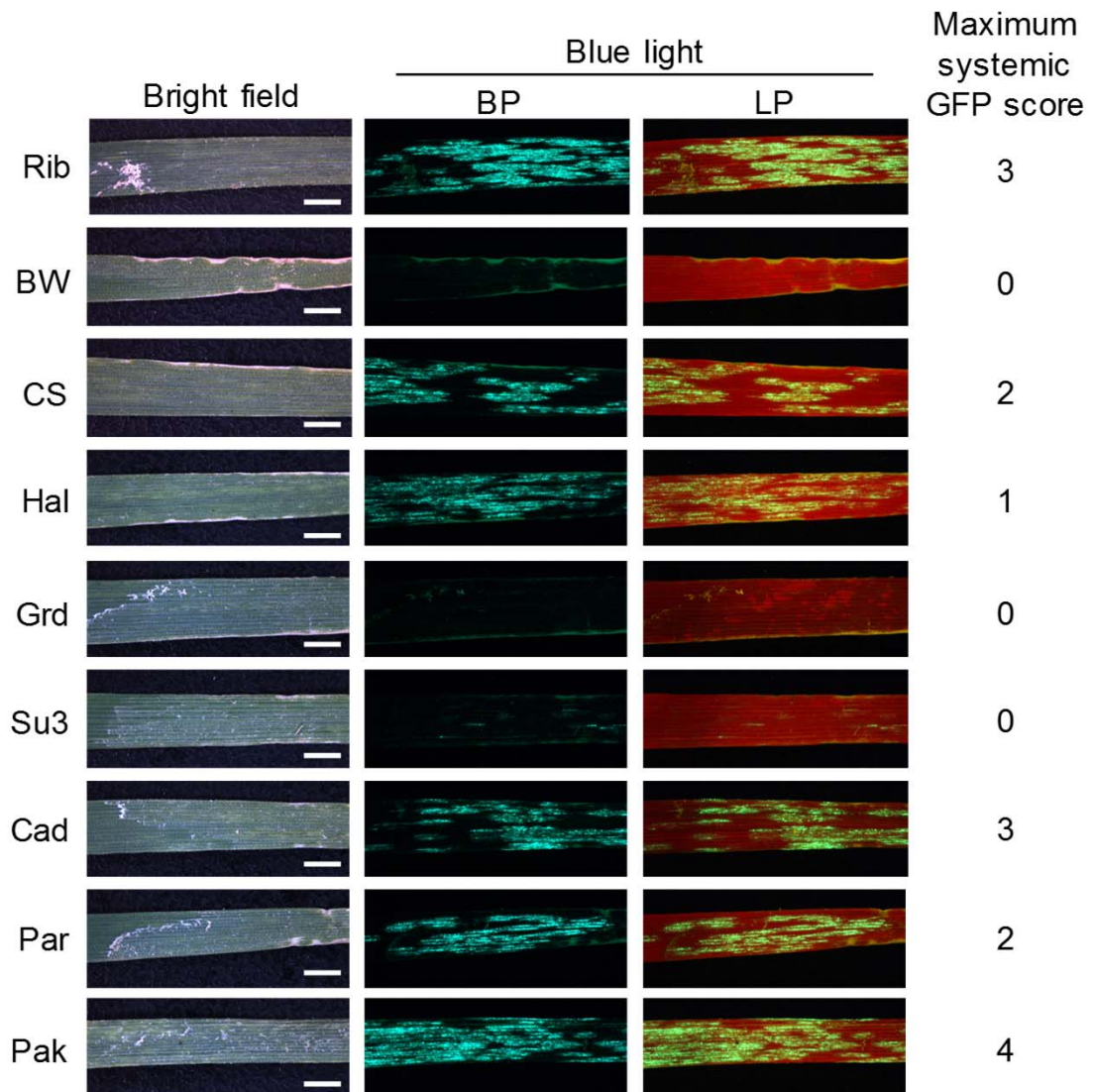
Figure 7. **Influence of the wheat genotype on FoMV-mediated protein expression.** PV101-GFP-inoculated leaves (L2) of different wheat cultivars photographed at 8-dpi using a fluorescence stereomicroscope mounted with bandpass (BP) and longpass (LP) filters. All fluorescence pictures were taken using identical acquisition settings. The maximum scores for GFP fluorescence coverage in systemically infected leaves of wheat cultivars Riband (Rib), Bobwhite (BW), Chinese Spring (CS), Halberd (Hal), Grandin (Grd), Sumai 3 (Su3), Cadenza (Cad), Paragon (Par), and Pakito (Pak) are indicated. Data are from at least 16 plants from 3 independent experiments. Bar = 2.5 mm.
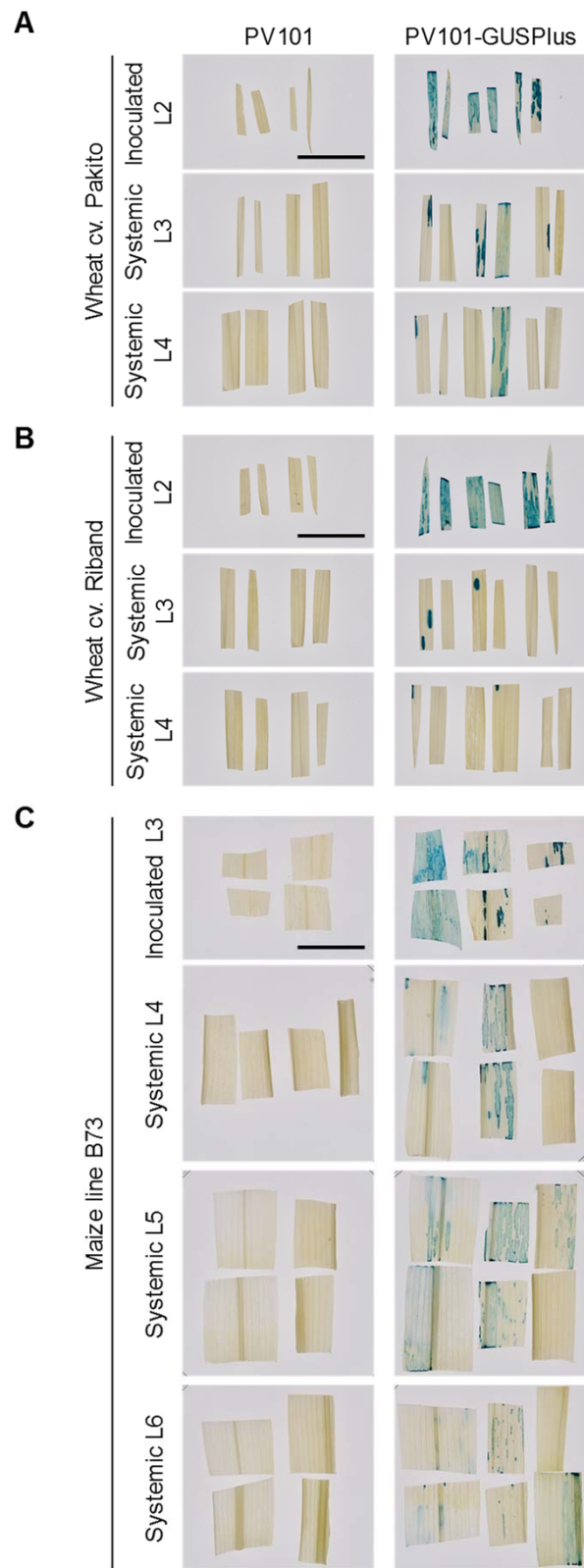
Figure 8. Expression of a 600 aa-long protein GUSPlus using a second generation FoMV vector PV101. PV101-GUSPlus was inoculated onto wheat cvs. Pakito **(A)** and Riband **(B)**, and onto maize line B73 **(C)** and GUSPlus activity in leaf samples from inoculated plants was detected by histochemical staining with X-Gluc. An empty vector PV101 was used as a control. Samples of inoculated leaves were taken at 9-dpi. Samples of first systemic wheat (L3) and maize (L4) leaves were taken at 15-dpi, and samples of second systemic wheat leaves (L4) and second and third maize leaves (L5 and L6) were taken at 22-dpi. Each leaf piece comes from a different individual plant. PV101- and PV101GUSPlus-infected material was sampled from 4 representative individuals from 2 independent experiments and from 6 representative individuals from 3 independent experiments, respectively. Bar = 20 mm.
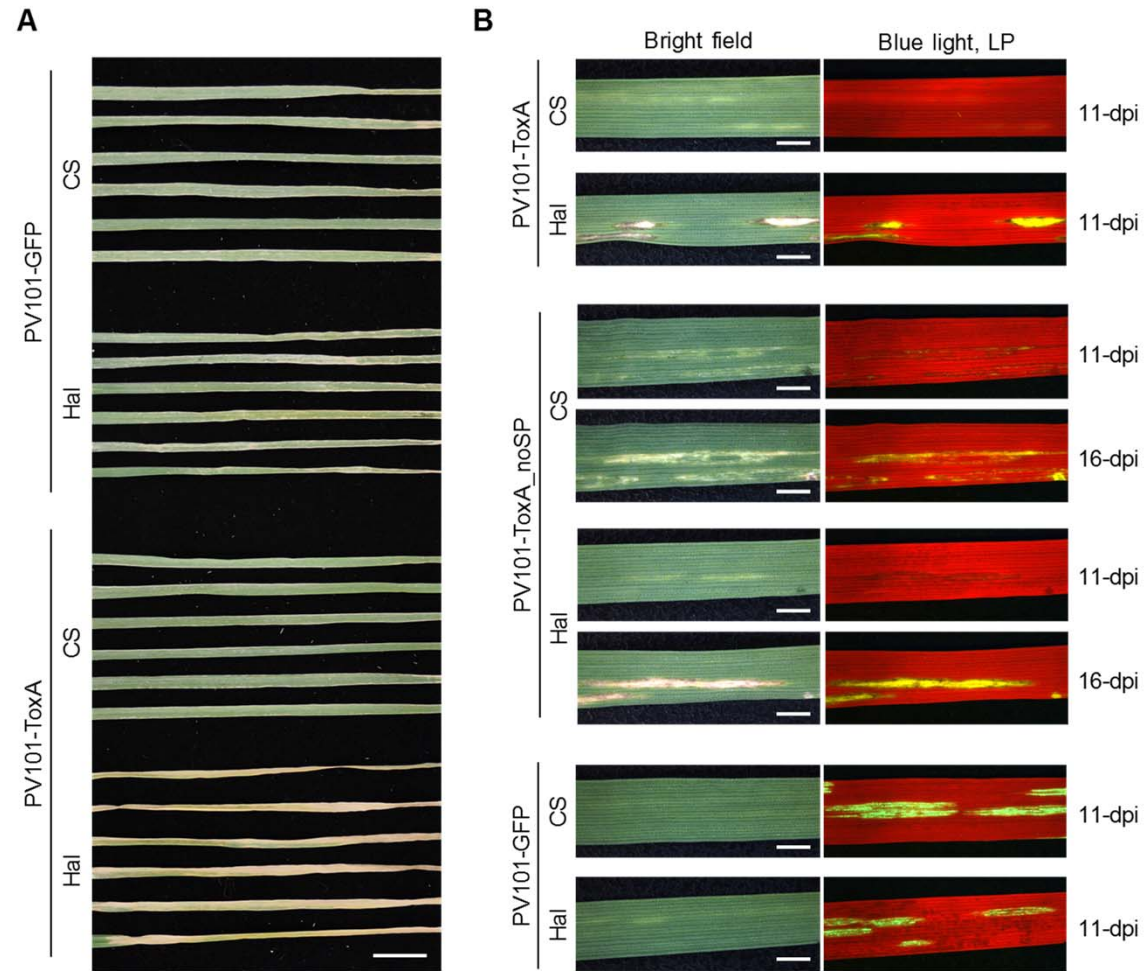
Figure 9. FoMV-mediated expression of a necrotrophic fungal effector ToxA from *Parastagonospora nodorum*.
A: PV101-GFP or PV101-ToxA inoculated leaves (L2) of wheat Chinese Spring, CS (ToxA insensitive) and Halberd, Hal (ToxA sensitive) seedlings at 6 dpi from one out of the two replicated experiments. Bar = 20 mm. **B:** Upper uninoculated leaves (L3) from wheat CS and Hal plants inoculated with PV101 carrying either full-length SnToxA effector protein with its native secretion signal peptide or its mature version without signal peptide (ToxA_noSP) at 11-dpi (and 16-dpi where indicated). Photographs were taken from the same leaf areas under white light or blue light using a fluorescence stereomicroscope mounted with a longpass filter (LP). Bar = 2.5 mm.

Parsed Citations

Broothaerts W, Mitchell HJ, Weir B, Kaines S, Smith LMA, Yang W, Mayer JE, Roa-Rodríguez C, Jefferson RA (2005) Gene transfer to plants by diverse species of bacteria. Nature 433: 629-633
Pubmed: Author and Title
CrossRef: Author and Title
Google Scholar: Author Only Title Only Author and Title

Brown RH, Hattersley PW (1989) Leaf anatomy of C3-C4 species as related to evolution of C4 photosynthesis. Plant Physiol 91: 1543-1550
Pubmed: Author and Title
CrossRef: Author and Title
Google Scholar: Author Only Title Only Author and Title

Chapman S, Kavanagh T, Baulcombe D (1992) Potato virus X as a vector for gene expression in plants. Plant J 2: 549-557
Pubmed: Author and Title
CrossRef: Author and Title
Google Scholar: Author Only Title Only Author and Title

Choi IR, Stenger DC, Morris TJ, French R (2000) A plant virus vector for systemic expression of foreign genes in cereals. Plant J 23: 547-555
Pubmed: Author and Title
CrossRef: Author and Title
Google Scholar: Author Only Title Only Author and Title

Csorba T, Burgyán J (2016) Antiviral silencing and suppression of gene silencing in plants. In A Wang, X Zhou, eds, Current Research Topics in Plant Virology. Springer International Publishing, Cham, pp 1-33
Pubmed: Author and Title
CrossRef: Author and Title
Google Scholar: Author Only Title Only Author and Title

Dagvadorj B, Ozketen AC, Andac A, Duggan C, Bozkurt TO, Akkaya MS (2017) A Puccinia striiformis f. sp. tritici secreted protein activates plant immunity at the cell surface. Sci Rep 7: 1141
Pubmed: Author and Title
CrossRef: Author and Title
Google Scholar: Author Only Title Only Author and Title

Dickmeis C, Fischer R, Commandeur U (2014) Potato virus X-based expression vectors are stabilized for long-term production of proteins and larger inserts. Biotechnol J 9: 1369-1379
Pubmed: Author and Title
CrossRef: Author and Title
Google Scholar: Author Only Title Only Author and Title

Domingo E, Sheldon J, Perales C (2012) Viral quasispecies evolution. Microbiol Mol Biol Rev 76: 159-216
Pubmed: Author and Title
CrossRef: Author and Title
Google Scholar: Author Only Title Only Author and Title

Faris JD, Zhang Z, Lu H, Lu S, Reddy L, Cloutier S, Fellers JP, Meinhardt SW, Rasmussen JB, Xu SS, Oliver RP, Simons KJ, Friesen TL (2010) A unique wheat disease resistance-like gene governs effector-triggered susceptibility to necrotrophic pathogens. Proc Natl Acad Sci USA 107: 13544-13549
Pubmed: Author and Title
CrossRef: Author and Title
Google Scholar: Author Only Title Only Author and Title

Franco-Orozco B, Berepiki A, Ruiz O, Gamble L, Griffe LL, Wang S, Birch PRJ, Kanyuka K, Avrova A (2017) A new proteinaceous pathogen-associated molecular pattern (PAMP) identified in Ascomycete fungi induces cell death in Solanaceae. New Phytol 214: 1657-1672
Pubmed: Author and Title
CrossRef: Author and Title
Google Scholar: Author Only Title Only Author and Title

Friesen TL, Stukenbrock EH, Liu ZH, Meinhardt S, Ling H, Faris JD, Rasmussen JB, Solomon PS, McDonald BA, Oliver RP (2006) Emergence of a new disease as a result of interspecific virulence gene transfer. Nat Gen 38: 953-956
Pubmed: Author and Title
CrossRef: Author and Title
Google Scholar: Author Only Title Only Author and Title

Hamilton CM (1997) A binary-BAC system for plant transformation with high-molecular-weight DNA. Gene 200: 107-116
Pubmed: Author and Title
CrossRef: Author and Title
Google Scholar: Author Only Title Only Author and Title

Harris RS (2007) Improved Pairwise Alignment of Genomic DNA. PhD Thesis, The Pennsylvania State University

CrossRef: Author and Title
Google Scholar: Author Only Title Only Author and Title

Heim R, Cubitt AB, Tsien RY (1995) Improved green fluorescence. Nature 373: 663-664

Pubmed: Author and Title
CrossRef: Author and Title
Google Scholar: Author Only Title Only Author and Title

Hellens RP, Edwards EA, Leyland NR, Bean S, Mullineaux PM (2000) pGreen: a versatile and flexible binary Ti vector for Agrobacterium-mediated plant transformation. Plant Mol Biol 42: 819-832

Pubmed: Author and Title
CrossRef: Author and Title
Google Scholar: Author Only Title Only Author and Title

Ji Q, Yang B, Lee M, Chen Y, Lubberstedt T (2010) Mapping of quantitative trait loci/locus conferring resistance to Foxtail mosaic virus in maize using the intermated B73 x Mo17 population. Plant Breed 129: 721-723

Pubmed: Author and Title
CrossRef: Author and Title
Google Scholar: Author Only Title Only Author and Title

Kettles GJ, Bayon C, Canning G, Rudd JJ, Kanyuka K (2017) Apoplastic recognition of multiple candidate effectors from the wheat pathogen Zymoseptoria tritici in the nonhost plant Nicotiana benthamiana. New Phytol 213: 338-350

Pubmed: Author and Title
CrossRef: Author and Title
Google Scholar: Author Only Title Only Author and Title

Kettles GJ, Bayon C, Sparks C, Canning G, Kanyuka K, Rudd JJ (2017) Characterisation of an antimicrobial and phytotoxic ribonuclease secreted by the fungal wheat pathogen Zymoseptoria tritici. New Phytol 217: 320-331

Pubmed: Author and Title
CrossRef: Author and Title
Google Scholar: Author Only Title Only Author and Title

Kreuze J (2014) siRNA Deep Sequencing and Assembly: Piecing Together Viral Infections. In ML Gullino, PJM Bonants, eds, Detection and Diagnostics of Plant Pathogens. Springer Netherlands, Dordrecht, pp 21-38

Pubmed: Author and Title
CrossRef: Author and Title
Google Scholar: Author Only Title Only Author and Title

Lacomme C, Santa Cruz S (1999) Bax-induced cell death in tobacco is similar to the hypersensitive response. Proc Natl Acad Sci USA 96: 7956-7961

Pubmed: Author and Title
CrossRef: Author and Title
Google Scholar: Author Only Title Only Author and Title

Langmead B, Salzberg SL (2012) Fast gapped-read alignment with Bowtie 2. Nat Methods 9: 357-359

Pubmed: Author and Title
CrossRef: Author and Title
Google Scholar: Author Only Title Only Author and Title

Lee WS, Hammond-Kosack KE, Kanyuka K (2012) Barley stripe mosaic virus-mediated tools for investigating gene function in cereal plants and their pathogens: Virus-induced gene silencing, Host-mediated gene silencing, and Virus-mediated overexpression of heterologous protein. Plant Physiol 160: 582-590

Pubmed: Author and Title
CrossRef: Author and Title
Google Scholar: Author Only Title Only Author and Title

Lee WS, Rudd JJ, Hammond-Kosack KE, Kanyuka K (2014) Mycosphaerella graminicola LysM effector-mediated stealth pathogenesis subverts recognition through both CERK1 and CEBiP homologues in wheat. Mol Plant Microbe Interact 27: 236-243

Pubmed: Author and Title
CrossRef: Author and Title
Google Scholar: Author Only Title Only Author and Title

Lin MK, Chang BY, Liao JT, Lin NS, Hsu YH (2004) Arg-16 and Arg-21 in the N-terminal region of the triple-gene-block protein 1 of Bamboo mosaic virus are essential for virus movement. J Gen Virol 85: 251-259

Pubmed: Author and Title
CrossRef: Author and Title
Google Scholar: Author Only Title Only Author and Title

Liu D, Shi L, Han C, Yu J, Li D, Zhang Y (2012) Validation of reference genes for gene expression studies in virus-infected Nicotiana benthamiana using quantitative real-time PCR. PLoS One 7: e46451

Pubmed: Author and Title
CrossRef: Author and Title
Google Scholar: Author Only Title Only Author and Title

Liu N, Xie K, Jia Q, Zhao JP, Chen TY, Li HG, Wei X, Diao XM, Hong YG, Liu YL (2016) Foxtail mosaic virus-induced gene silencing in

monocot plants. Plant Physiol 171: 1801-1807

Pubmed: Author and Title
CrossRef: Author and Title
Google Scholar: Author Only Title Only Author and Title

Liu Z, Friesen TL, Ling H, Meinhardt SW, Oliver RP, Rasmussen JB, Faris JD (2006) The Tsn1-ToxA interaction in the wheat-Stagonospora nodorum pathosystem parallels that of the wheat-tan spot system. Genome 49: 1265-1273

Pubmed: Author and Title
CrossRef: Author and Title
Google Scholar: Author Only Title Only Author and Title

Liu Z, Kearney CM (2010) An efficient Foxtail mosaic virus vector system with reduced environmental risk. BMC Biotechnol 10: 88

Pubmed: Author and Title
CrossRef: Author and Title
Google Scholar: Author Only Title Only Author and Title

Lu R, Malcuit I, Moffett P, Ruiz MT, Peart J, Wu AJ, Rathjen JP, Bendahmane A, Day L, Baulcombe DC (2003) High throughput virus-induced gene silencing implicates heat shock protein 90 in plant disease resistance. EMBO J 22: 5690-5699

Pubmed: Author and Title
CrossRef: Author and Title
Google Scholar: Author Only Title Only Author and Title

Luo RB, Liu BH, Xie YL, Li ZY, Huang WH, Yuan JY, He GZ, Chen YX, Pan Q, Liu YJ, Tang JB, Wu GX, Zhang H, Shi YJ, Liu Y, Yu C, Wang B, Lu Y, Han CL, Cheung DW, Yiu SM, Peng SL, Zhu XQ, Liu GM, Liao XK, Li YR, Yang HM, Wang J, Lam TW, Wang J (2012) SOAPdenovo2: an empirically improved memory-efficient short-read de novo assembler. Gigascience 1: 6

Pubmed: Author and Title
CrossRef: Author and Title
Google Scholar: Author Only Title Only Author and Title

Majer E, Llorente B, Rodriguez-Concepcion M, Daros JA (2017) Rewiring carotenoid biosynthesis in plants using a viral vector. Sci Rep 7: 10

Pubmed: Author and Title
CrossRef: Author and Title
Google Scholar: Author Only Title Only Author and Title

Manning VA, Chu AL, Scofield SR, Ciuffetti LM (2010) Intracellular expression of a host-selective toxin, ToxA, in diverse plants phenocopies silencing of a ToxA-interacting protein, ToxABP1. New Phytol 187: 1034-1047

Pubmed: Author and Title
CrossRef: Author and Title
Google Scholar: Author Only Title Only Author and Title

Manning VA, Ciuffetti LM (2005) Localization of Ptr ToxA produced by Pyrenophora tritici-repentis reveals protein import into wheat mesophyll cells. Plant Cell 17: 3203-3212

Pubmed: Author and Title
CrossRef: Author and Title
Google Scholar: Author Only Title Only Author and Title

Mei Y, Zhang CQ, Kernodle BM, Hill JH, Whitham SA (2016) A Foxtail mosaic virus vector for Virus-induced gene silencing in maize. Plant Physiol 171: 760-772

Pubmed: Author and Title
CrossRef: Author and Title
Google Scholar: Author Only Title Only Author and Title

Meng Y, Moscou MJ, Wise RP (2009) Blufensin1 negatively impacts basal defense in response to barley powdery mildew. Plant Physiol 149: 271-285

Pubmed: Author and Title
CrossRef: Author and Title
Google Scholar: Author Only Title Only Author and Title

Nakamura S, Mano S, Tanaka Y, Ohnishi M, Nakamori C, Araki M, Niwa T, Nishimura M, Kaminaka H, Nakagawa T, Sato Y, Ishiguro S (2010) Gateway binary vectors with the bialaphos resistance gene, bar, as a selection marker for plant transformation. Biosci Biotechnol Biochem 74: 1315-1319

Pubmed: Author and Title
CrossRef: Author and Title
Google Scholar: Author Only Title Only Author and Title

Panwar V, McCallum B, Bakkeren G (2013) Endogenous silencing of Puccinia triticina pathogenicity genes through in planta-expressed sequences leads to the suppression of rust diseases on wheat. Plant J 73: 521-532

Pubmed: Author and Title
CrossRef: Author and Title
Google Scholar: Author Only Title Only Author and Title

Paolacci AR, Tanzarella OA, Porceddu E, Ciaffi M (2009) Identification and validation of reference genes for quantitative RT-PCR normalization in wheat. BMC Mol Biol 10: 27

Pubmed: Author and Title

CrossRef: Author and Title
Google Scholar: Author Only Title Only Author and Title

Paulsen AQ, Niblett CL (1977) Purification and properties of Foxtail mosaic virus. Phytopathology 67: 1346-1351

Pubmed: Author and Title
CrossRef: Author and Title
Google Scholar: Author Only Title Only Author and Title

Robertson NL, French R, Morris TJ (2000) The open reading frame 5A of Foxtail mosaic virus is expressed in vivo and is dispensable for systemic infection. Arch Virol 145: 1685-1698

Pubmed: Author and Title
CrossRef: Author and Title
Google Scholar: Author Only Title Only Author and Title

Schnable PS, Ware D, Fulton RS, Stein JC, Wei F, Pasternak S, Liang C, Zhang J, Fulton L, Graves TA, Minx P, Reily AD, Courtney L, Kruchowski SS, Tomlinson C, Strong C, Delehaunty K, Fronick C, Courtney B, Rock SM, Belter E, Du F, Kim K, Abbott RM, Cotton M, Levy A, Marchetto P, Ochoa K, Jackson SM, Gillam B, Chen W, Yan L, Higginbotham J, Cardenas M, Waligorski J, Applebaum E, Phelps L, Falcone J, Kanchi K, Thane T, Scimone A, Thane N, Henke J, Wang T, Ruppert J, Shah N, Rotter K, Hodges J, Ingenthron E, Cordes M, Kohlberg S, Sgro J, Delgado B, Mead K, Chinwalla A, Leonard S, Crouse K, Collura K, Kudrna D, Currie J, He R, Angelova A, Rajasekar S, Mueller T, Lomeli R, Scara G, Ko A, Delaney K, Wissotski M, Lopez G, Campos D, Braidotti M, Ashley E, Golser W, Kim H, Lee S, Lin J, Dujmic Z, Kim W, Talag J, Zuccolo A, Fan C, Sebastian A, Kramer M, Spiegel L, Nascimento L, Zutavern T, Miller B, Ambroise C, Muller S, Spooner W, Narechania A, Ren L, Wei S, Kumari S, Faga B, Levy MJ, McMahan L, Van Buren P, Vaughn MW, Ying K, Yeh CT, Emrich SJ, Jia Y, Kalyanaraman A, Hsia AP, Barbazuk WB, Baucom RS, Brutnell TP, Carpita NC, Chaparro C, Chia JM, Deragon JM, Estill JC, Fu Y, Jeddeloh JA, Han Y, Lee H, Li P, Lisch DR, Liu S, Liu Z, Nagel DH, McCann MC, SanMiguel P, Myers AM, Nettleton D, Nguyen J, Penning BW, Ponnala L, Schneider KL, Schwartz DC, Sharma A, Soderlund C, Springer NM, Sun Q, Wang H, Waterman M, Westerman R, Wolfgruber TK, Yang L, Yu Y, Zhang L, Zhou S, Zhu Q, Bennetzen JL, Dawe RK, Jiang J, Jiang N, Presting GG, Wessler SR, Aluru S, Martienssen RA, Clifton SW, McCombie WR, Wing RA, Wilson RK (2009) The B73 maize genome: complexity, diversity, and dynamics. Science 326: 1112-1115

Pubmed: Author and Title
CrossRef: Author and Title
Google Scholar: Author Only Title Only Author and Title

Seguin J, Rajeswaran R, Malpica-Lopez N, Martin RR, Kasschau K, Dolja VV, Otten P, Farinelli L, Pooggin MM (2014) De novo reconstruction of consensus master genomes of plant RNA and DNA viruses from siRNAs. PLoS One 9: 8

Pubmed: Author and Title
CrossRef: Author and Title
Google Scholar: Author Only Title Only Author and Title

Seifers DL, Harvey TL, Haber S, She YM, Chernushevich I, Ens W, Standing KG (1999) Natural infection of sorghum by Foxtail mosaic virus in Kansas. Plant Dis 83: 905-912

Pubmed: Author and Title
CrossRef: Author and Title
Google Scholar: Author Only Title Only Author and Title

Sempere RN, Gomez P, Truniger V, Aranda MA (2011) Development of expression vectors based on Pepino mosaic virus. Plant Methods 7: 6

Pubmed: Author and Title
CrossRef: Author and Title
Google Scholar: Author Only Title Only Author and Title

Silva D, Santos G, Barroca M, Collins T (2017) Inverse PCR for point mutation introduction. Methods Mol Biol 1620: 87-100

Pubmed: Author and Title
CrossRef: Author and Title
Google Scholar: Author Only Title Only Author and Title

Sztuba-Solińska J, Stollar V, Bujarski JJ (2011) Subgenomic messenger RNAs: Mastering regulation of (+)-strand RNA virus life cycle. Virology 412: 245-255

Pubmed: Author and Title
CrossRef: Author and Title
Google Scholar: Author Only Title Only Author and Title

Tang C, Wei J, Han Q, Liu R, Duan X, Fu Y, Huang X, Wang X, Kang Z (2015) PsANT, the adenine nucleotide translocase of Puccinia striiformis, promotes cell death and fungal growth. Sci Rep 5: 11241

Pubmed: Author and Title
CrossRef: Author and Title
Google Scholar: Author Only Title Only Author and Title

Tatineni S, McMechan AJ, Bartels M, Hein GL, Graybosch RA (2015) In vitro transcripts of wild-type and fluorescent protein-tagged Triticum mosaic virus (family Potyviridae) are biologically active in wheat. Phytopathology 105: 1496-1505

Pubmed: Author and Title
CrossRef: Author and Title
Google Scholar: Author Only Title Only Author and Title

Tatineni S, McMechan AJ, Hein GL, French R (2011) Efficient and stable expression of GFP through Wheat streak mosaic virus-based vectors in cereal hosts using a range of cleavage sites: Formation of dense fluorescent aggregates for sensitive virus tracking.

Virology 410: 268-281
Pubmed: Author and Title
CrossRef: Author and Title
Google Scholar: Author Only Title Only Author and Title

Xu W, Meng Y, Surana P, Fuerst G, Nettleton D, Wise RP (2015) The knottin-like Blufensin family regulates genes involved in nuclear import and the secretory pathway in barley-powdery mildew interactions. Front Plant Sci 6: 409
Pubmed: Author and Title
CrossRef: Author and Title
Google Scholar: Author Only Title Only Author and Title

Yuan C, Li C, Yan L, Jackson AO, Liu Z, Han C, Yu J, Li D (2011) A high throughput Barley stripe mosaic virus vector for virus induced gene silencing in monocots and dicots. PLoS One 6: e26468
Pubmed: Author and Title
CrossRef: Author and Title
Google Scholar: Author Only Title Only Author and Title

Zerbino DR (2010) Using the Velvet de novo assembler for short-read sequencing technologies. Curr Protoc Bioinformatics Chapter 11: Unit 11.5
Pubmed: Author and Title
CrossRef: Author and Title
Google Scholar: Author Only Title Only Author and Title

Zhang H, Wang L, Hunter D, Voogd C, Joyce N, Davies K (2013) A Narcissus mosaic viral vector system for protein expression and flavonoid production. Plant Methods 9: 28
Pubmed: Author and Title
CrossRef: Author and Title
Google Scholar: Author Only Title Only Author and Title

Zhang J, Yu DS, Zhang Y, Liu K, Xu KD, Zhang FL, Wang J, Tan GX, Nie XH, Ji QH, Zhao L, Li CW (2017) Vacuum and co-cultivation Agroinfiltration of (germinated) seeds results in Tobacco rattle virus (TRV) mediated whole-plant virus-induced gene silencing (VIGS) in wheat and maize. Front Plant Sci 8: 393
Pubmed: Author and Title
CrossRef: Author and Title
Google Scholar: Author Only Title Only Author and Title